Transactions of the I·R·E

Professional Group on Antennas and Propagation

VOLUME AP-I NUMBER 1 JULY 1953
Published Quarterly

The Institute of Radio Engineers

TRANSACTIONS OF THE I.R.E.®

PROFESSIONAL GROUP ON ANTENNAS AND PROPAGATION

A QUARTERLY PUBLICATION DEVOTED TO EXPERIMENTAL AND THEORETICAL PAPERS ON ANTENNAS AND WIRELESS PROPAGATION OF ELECTROMAGNETIC WAVES

The Professional Group on Antennas and Propagation is an organization, within the framework of the IRE, of members with principal professional interest in Antennas and Propagation. All Members of the IRE are eligible for membership in the Group and will receive all Group publications upon payment of prescribed assessments.

Annual Assessment: $4.00

MANUSCRIPTS should be submitted to John B. Smyth, Editor, U. S. Navy Electronics Laboratory, San Diego, California. Manuscripts should be original typewritten copy, double spaced, plus one carbon copy. References should appear as footnotes and include author's name, title, journal, volume, initial and final page numbers, and date. Each paper must have an abstract of not more than 200 words.

ILLUSTRATIONS should be submitted as follows: All line drawings (graphs, charts, block diagrams, cutaways, etc.) should be inked uniformly and ready for reproduction. If commercially printed grids are used in graph drawings, author should be sure printer's ink is of a color that will reproduce. All half-tone illustrations (photographs, wash, airbrush, or pencil renderings, etc.) should be clean and ready to reproduce. Photographs should be glossy prints. Call-outs or labels should be marked on a registered tissue overlay, not on the illustration itself. No illustration should be larger than 8 x 10 inches.

Copies can be purchased from

THE INSTITUTE OF RADIO ENGINEERS
1 East 79 Street, New York 21, N.Y.

PRICE PER COPY: members of the Professional Group on Antennas and Propagation $1.20; members of the IRE $1.80; nonmembers $3.60.

Application has been made for second class entry, at the post office at Menasha, Wisconsin, under the act of March 3, 1879. Acceptance for mailing at a special rate of postage is provided for in the act of February 28, 1925, embodied in Paragraph 4, Section 412, P. L. and R., authorized October 26, 1927.

news and views

WITH this issue, the TRANSACTIONS of the PGAP formally establishes itself as the organized technical publication of the membership. The technical papers that will be presented in this quarterly journal will have undergone the same careful and discriminating attention customarily accorded to papers published in the PROCEEDINGS. With the wholehearted support and cooperation of the Institute, we expect to see this new quarterly take its place as the official technical organ for the workers in the Antenna and Propagation field.

This section—*News and Views*—of the TRANSACTIONS will be a regular feature in each issue. Here, too, we hope to work out the problems of the Group by free discussion, welcoming free criticism as well as praise. We wish to use this section, in part, as a medium for ironing out controversial issues, a forum where the membership may feel free to express itself.

A matter that we should like to bring to the attention of the Group covers the whole general subject of the form and organization of the professional groups—how many should there be, and how broad a field should each cover. The present organization reflects the thinking of a relatively small handful of energetic people who started with the basic premise that the Institute *per se* had grown much too big to satisfy the specialized needs of blocks of engineers. There is little doubt as to the wisdom of this basic premise. However, are the professional groups, as currently constituted, properly and cohesively subdivided?

Listed below are the twenty-one professional groups recognized currently by the Institute. Truly, the IRE is going through a period of transition.

Airborne Electronics
Antennas & Propagation
Audio
Broadcast & Television Receivers
Broadcast Transmission Systems
Circuit Theory
Communications Systems
Component Parts
Electron Devices
Electronic Computers
Engineering Management
Industrial Electronics
Information Theory
Instrumentation
Medical Electronics
Microwave Theory & Techniques
Nuclear Science
Quality Control
Radio Telemetry & Remote Control
Vehicular Communication
Ultrasonics

As an example of one opinion, we have received the following letter from Mr. Harold Wheeler of Wheeler Laboratories. His letter is reproduced here just as received:

"The time-honored association of Antennas and Propagation in IRE Committees has now outlived its usefulness. This has become more and more apparent when we note the striking division of interests within the Professional Group on Antennas and Propagation.

"Therefore I propose that this Professional Group be split into two separate groups to be designated as follows:

Professional Group on Radio Antennas
Professional Group on Radio Propagation

"I think the need for such a separation will be apparent to anyone who is familiar with the group and thoughtfully considers the question. If you should find a diversity of opinion on this question of separation, then I should like to have an opportunity to argue the point.

"It would be most beneficial if this separation could be made as soon as possible."

Here is a point of view that argues that the current subdivisions are not specialized enough. On the other hand, we are sure that there are many of the membership who feel that the present subdivision is already too fine.

As one result of the formation of twenty-one separate professional groups, we now find a great increase in the number of technical meetings and conventions; more papers are being presented and published, with wider geographical distribution than ever before. The availability of organizing personnel in each professional group for sponsoring such meetings has provided this enlarged activity. But as with so many things, this may have its vices as well as its virtues.

While it may well be that greater subdivision results in greater progress in each specialized area, it may equally well be that in the effort to nurture each further subdivision, the resulting wheat becomes increasingly indiscernible from the chaff. Then there is the problem of broad coordination of these various specialities. These are the questions vital to all of us in the IRE.

We welcome your views for frank discussion.

Organization

PGAP Administrative Committee

The operation of the Professional Group on Antennas and Propagation is under the guidance of the Administrative Committee, as follows:

Chairman:
Dr. A. H. Waynick
The Pennsylvania State College
State College, Pennsylvania

Vice-Chairman:
Mr. P. S. Carter
RCA Laboratories Division
Rocky Point, L. I., N. Y.

Secretary-Treasurer:
Mr. Delmer C. Ports
Jansky and Bailey
Washington 7, D. C.

Administrative Committee Members:
Dr. George Sinclair
Sinclair Radio Laboratories, Ltd.
Toronto, Canada

Dr. J. B. Smyth
U. S. Navy Electronics Laboratory
San Diego 52, Calif.

Dr. H. G. Booker
School of Electrical Engineering
Cornell University
Ithaca, N. Y.

Mr. H. M. Wells
Carnegie Institute of Washington
Washington 15, D. C.

Dr. L. C. Van Atta
Research and Development Laboratories
Hughes Aircraft Company
Culver City, Calif.

Dr. L. J. Chu
Department of Electrical Engineering
Massachusetts Institute of Technology
Cambridge 39, Mass.

Ex Officio Members:
H. A. Finke
Polytechnic Research & Development Co.
Brooklyn 1, N. Y.

J. S. Brown
Andrew Corporation
Chicago 19, Ill.

Robert B. Jacques
Electronics Division
Thompson Products, Inc.
Cleveland 14, Ohio

PGAP Officers for 1953–54

Mr. P. C. Carter has been elected as Chairman and Mr. D. C. Ports as Vice-Chairman for the year beginning June 1, 1953. The position of Secretary-Treasurer is open for the moment but will be filled very shortly.

Membership

All IRE members whose interest lies in the field of Antennas and Propagation are eligible for membership in the PGAP and will receive the TRANSACTIONS and all other group publications upon payment of the current assessment of $4.00 per year. The assessment is the Group's principal means of covering the cost of the TRANSACTIONS. The TRANSACTIONS is sent to paid up members only. A glance at the present, initial issue should convince unpaid members that they would be missing a valuable contribution to their field of interest.

Transactions

The aim of the TRANSACTIONS is to serve as a professional organ to meet and integrate the needs of the membership.

Contributed papers are given the same careful examination as contributions to the PROCEEDINGS receive. The more restricted area of the TRANSACTIONS permit a prompt consideration of all papers.

Dr. E. Weber, Chairman of the IRE Awards Committee has indicated to us that papers which appear in Professional Group Transactions will be considered along with papers appearing in the PROCEEDINGS OF THE I.R.E. in connection with awards, such as the B. J. Thompson Award. The Executive Committee of the IRE also is considering setting up a policy wherein a $100.00 award would be given for the best paper presented each year in each Professional Groups' Transactions.

It is hoped that the membership will take an active part in the success of our journal. Contributions are invited.

The diagram on the following page shows the administrative organization of the TRANSACTIONS.

Group Chapters and Chapter News

At the "grass roots" level, the professional group chapters should be the key to maintaining an active interest in the PGAP as a whole. In certain sections of the IRE where great interest in antennas and propagation is concerned, group chapters have been formed, are being formed, or their possibility considered. PGAP members often, while realizing the value of such "grass roots" meetings and technical sessions, fail to lend their energies in making local group meetings worthwhile and productive.

Chapters have been established in Chicago and Los Angeles. Other chapters in the process of being formed are in the New York area, San Diego, and San Francisco. PGAP members are urged to enter the activities of these chapters, and in areas where chapter activities have not yet reached an organized stage, to investigate the ways and means for getting one going. J. S. Brown, Group Membership Chairman, stands ready to lend an accomplished hand in this matter.

Administrative Committee of the Professional Group on Antennas and Propagation

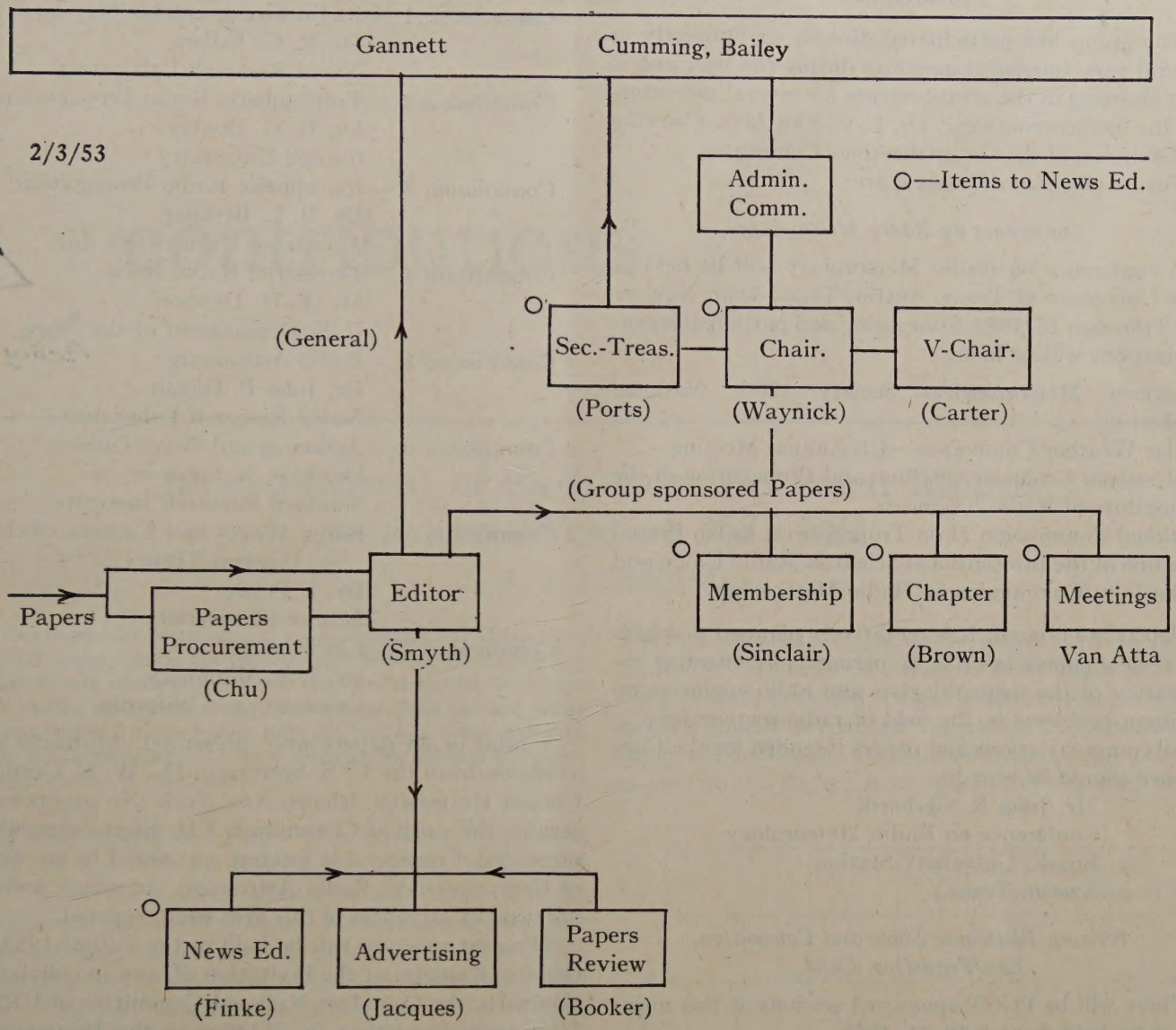

Chapter News

Los Angeles. At the April 17 meeting of the chapter, attended by 62 persons, the following IRE Antenna and Propagation officers were elected:

Chairman: Dr. M. J. Ehrlich
Research Development Labs.
Hughes Aircraft Co.
Culver City, Calif.

Vice-Chairman: Dr. R. S. Wehner
Research and Development Labs.
Hughes Aircraft Co.
Culver City, Calif.

Secretary: Mr. Robert Krausz
Microwave Engineering Co.
4000 Mount Lee Drive
Los Angeles 28, Calif.

At this same meeting, Dr. John V. N. Granger of Stanford Research Institute gave a general talk on "Aircraft Antenna Design Limitations."

Chicago. The following chapter officers were elected at the February meeting:

Chairman: G. Kearse
American Phenolic Corporation

Vice-Chairman: L. R. Krahe
Andrew Corporation

Secretary: R. A. Jensen
Sears Roebuck & Co.

They will take office on July 1.

The following chapter meetings and talks have been held during the past season:

Oct. 17 —"Antenna Design for Microwave Relays," by E. Dyk, Motorola, Inc.

Nov. 21—"UHF Measurements and Smith Chart," by Joseph Markin, Raytheon.

Feb. 20 —"The Corner Reflector Antenna," by E. Harris, Mark Products Co.

Apr. 17 —"Antenna Problems in Air Navigation," by S. Rachie, C. A. C.

Meetings

The group has participated directly or indirectly in several very successful meetings during the year and is now assisting in the arrangements for several more during the forthcoming year. Dr. L. C. Van Atta is serving as Chairman of the Group meetings Committee.

Future meetings of interest are:

Conference on Radio Meteorology

A conference on Radio Meteorology will be held at The University of Texas, Austin, Texas, from November 9 through 12, 1953. Sponsoring and participating organizations will include:

American Meteorological Society—126th National Meeting.
Radar Weather Conference—4th Annual Meeting.
Professional Group on Antennas and Propagation of the Institute of Radio Engineers.
National Commission II on Tropospheric Radio Propagation of the International Scientific Radio Union and the Joint Commission on Radio Meteorology.

Papers are invited. It is tentatively planned to schedule review papers in order to permit more effective cooperation of the meteorologists and radio engineers on common problems in the field of radio meteorology.

All communications and papers intended for the Conference should be sent to:

Mr. John R. Gerhardt
Conference on Radio Meteorology
Box F, University Station
Austin, Texas.

Western Electronic Show and Convention, San Francisco, Calif.

There will be PGAP sponsored sessions at this meeting to be held August 19–21, 1953.

U. S. A. National Committee URSI Spring Meeting, 1953

(In collaboration with the I.R.E. Professional Group on Antennas and Propagation)

An attendance of approximately 350 was obtained at the Spring 1953 meeting of the U.S.A. National Committee of URSI, in collaboration with the I.R.E. Professional Group on Antennas and Propagation, held at the National Bureau of Standards, Washington, D. C. on April 27, 28, 29, and 30, 1953.

The U.S.A. National Committee met on April 30, 1953, and elected Officers for the years 1953–1955. The new officers are listed:

Chairman:	Dr. A. H. Waynick Pennsylvania State College
Vice-Chairman:	Mr. H. W. Wells Carnegie Inst. of Washington
Secretary-Treasurer:	Dr. W. E. Gordon Cornell University

Commission Chairmen:

Commission 1 —Radio Measurements Standards:
Dr. R. G. Fellers
Naval Research Laboratory

Commission 2 —Tropospheric Radio Propagation:
Dr. H. G. Booker
Cornell University

Commission 3 —Ionospheric Radio Propagation:
Dr. B. L. Berkner
Associated Universities, Inc.

Commission 4 —Terrestrial Radio Noise:
Mr. F. H. Dickson
U. S. Department of the Navy

Commission 5 —Radio Astronomy:
Dr. John P. Hagan
Naval Research Laboratory

Commission 6a—Antennas and Wave Guides:
Dr. J. V. N. Granger
Stanford Research Institute

Commission 6b—Radio Waves and Circuits, Including General Theory:
Dr. J. Pettit
Stanford University

Commission 7 —Electronics:
Dr. J. R. Whinnery
University of California

A total of 83 papers were presented. Abstracts are available from the U. S. Secretary, Dr. W. E. Gordon, Cornell University, Ithaca, New York. No papers concerning the work of Commission VII, Electronics, were presented. Considerable interest was noted in the work of Commission V, Radio Astronomy, in which several noteworthy advances in this field were reported.

The next meeting will be held in the Fall of 1953 at Ottawa, Canada, at the invitation of, and in collaboration with, the Canadian National Committee of URSI. It is anticipated that in addition to the Professional Groups on Antennas and Propagation, other I.R.E. Professional Groups will also participate in this meeting.

A listing of the commissions and papers which were presented under their sponsorship follows:

Combined Session of Participating U.S.A. National Commissions

Remarks concerning the Xth General Assembly of URSI, Sydney, Australia, August, 1952—C. R. Burrows, Chairman, U.S.A. National Committee of URSI, Cornell University, Ithaca, New York.

Auroral Research at the Geophysical Institute, University of Alaska—C. T. Elvey, University of Alaska, College, Alaska.

The Probability Distribution of Atmospheric Noise—A. W. Sullivan, J. M. Barney and S. P. Hersperger, University of Florida, Gainesville, Florida.

Interstellar 21 CM Radiation—H. I. Ewen, Harvard University, Cambridge, Massachusetts.

Effects of the Moon on the Outer Atmosphere—A. G. McNish, Nat'l. Bureau of Standards, Washington, D. C.

contributions

Measurement of Path Loss Between Miami and Key West at 3675 MC

R. L. ROBBINS*

Summary—**Radio transmission measurements have been made at 3675 megacycles on the 130-mile path between Miami and Key West, Florida, which is largely over watery wastes of the Everglades and shallow sea waters of the Florida Keys. Path loss and fading characteristics for this terrain were not found to differ materially from the characteristics of hilly or mountainous paths in the northeastern section of the country.**

THE PROPAGATION of microwave frequencies to distances far beyond the optical horizon has been the subject of considerable study and experimentation in recent years. K. Bullington[1] has summarized the principal findings published and has added data obtained by the Bell Telephone Laboratories over the rolling and mountainous terrain found in the North Atlantic and New England states. During September 1952, the Laboratories conducted similar tests of 3675-mc propagation over a 130-mile path between Miami and Key West, Florida, where the transmission path was largely over the watery wastes of the Everglades and the shallow Gulf of Mexico waters north of the Florida Keys. Somewhat less than fifteen per cent of the path was over dry land.

Fig. 1 is a mass plot of all the available data on the median signal levels measured at various distances from the transmitter. The triangles represent previous findings and the dots represent data taken in Florida.

The tests were conducted over five transmission paths, varying in length from 123 to 138 miles, between three transmitting sites in the vicinity of Miami and three receiving sites at Key West. The sites chosen provided various foregrounds; i.e., water, relatively light vegetation over smooth ground and the roof tops of residences.

The first transmitting site, on the property of the Tropical Radio Telegraph Co. about 13 miles north of downtown Miami, provided a clear transmission path over smooth ground having low vegetation for a distance of about one-half mile. The second transmitting site was located on the Rickenbacker Causeway adjacent to the island of Virginia Key. The smooth waters of Biscayne Bay extended southward from the very base of the tower for eight miles. The third transmitting site, at the western border of Coral Gables, was on the roof of the "87" Exchange Building of the Southern Bell Telephone and

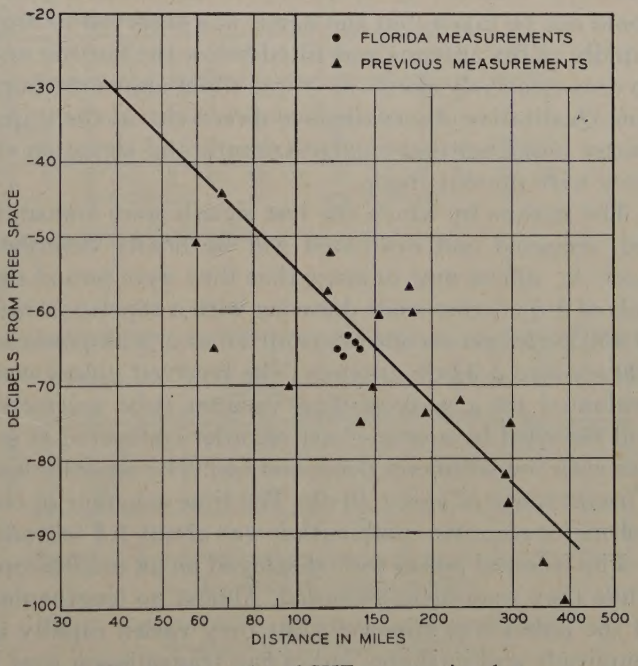

Fig. 1—Mass plot of SHF propagation data.

* Bell Telephone Labs., Inc., New York, N. Y.

[1] K. Bullington, "Radio transmission beyond the horizon in the 40- to 4000-mc band," PROC. I.R.E., pp. 132–135; January, 1953.

Telegraph Company where the transmission path was over the neighboring residences. The antenna was about forty-five feet above the ground.

The first Key West receiving site was at the western edge of the Municipal Golf Course. The smooth mangrove-covered rocky terrain sloped gently into the water. The second receiving site was located on Bertha St. near the Atlantic Ocean. Here the signals arrived over the smooth shallow waters of a former salt evaporating pond and a group of residences about one mile away. The antenna tower was erected on level coral fill about 75 feet from the water. The third receiving site was on the roof of the La Concha Hotel. The building is six stories high and the roof is well above the surrounding business buildings and residences.

Fair weather, except for small scattered thunderstorms prevailed at both Miami and Key West during the period of the test. It is believed that similar weather existed between the two cities. The storms varied from light to sharp intensity.

The received signals were observed and recorded for a period of approximately forty-eight hours during each test. As ascertained by observation of the receiving antenna alignment and of a magnetic compass, the signals were approaching over a great circle path. A $\pm 4°$ azimuth adjustment of the 57-inch paraboloid receiving antenna (32 db gain) was required to reduce the received signal strength by 3 db. Such an antenna has a nominal beam width of 3.5° between the half-power points. A measure of directivity in the vertical plane could not be taken, but the signal was observed to drop rapidly as the antenna was tilted below the horizon and to drop relatively slowly as it was tilted above the horizon. Qualitative observations of directivity at the transmitter indicated that similar azimuth and elevation effects were present there.

The mieans by which the test signals were transmitted, recesved and evaluated will be briefly described later. It uffices now to know that they were pulsed signals of 1·5 microseconds duration with a repetition rate of 400 cycles per second transmitted at a peak power of 500 kw into a 32-db antenna. The received pulses were evaluated by a peak-reading vacuum tube voltmeter and recorded by a strip-chart recorder connected in series with the voltmeter deflection coil. The recorder had a useful range of about 10 db. The time constant of the voltmeter-recorder combination was about 1.5 seconds.

The received pulses were displayed on an oscilloscope while they were being recorded. Almost no lengthening of the pulses was observed; but they varied rapidly in amplitude and in shape, indicating transmission over a multiplicity of paths. Many of the fluctuations were probably too fast to be caught by eye.

A typical strip-chart recording of the pulses is shown in Fig. 2. The lower portion of the chart was recorded at a speed of 15 minutes per division, or 3 inches per hour. The upper portion was recorded at a speed of 15 seconds per division, or 3 inches per minute, to expand the time scale. A calibration scale has been superimposed at the bottom of the chart. It is seen that the pulse amplitude, as recorded, varied approximately ± 2 db about a short-term average.

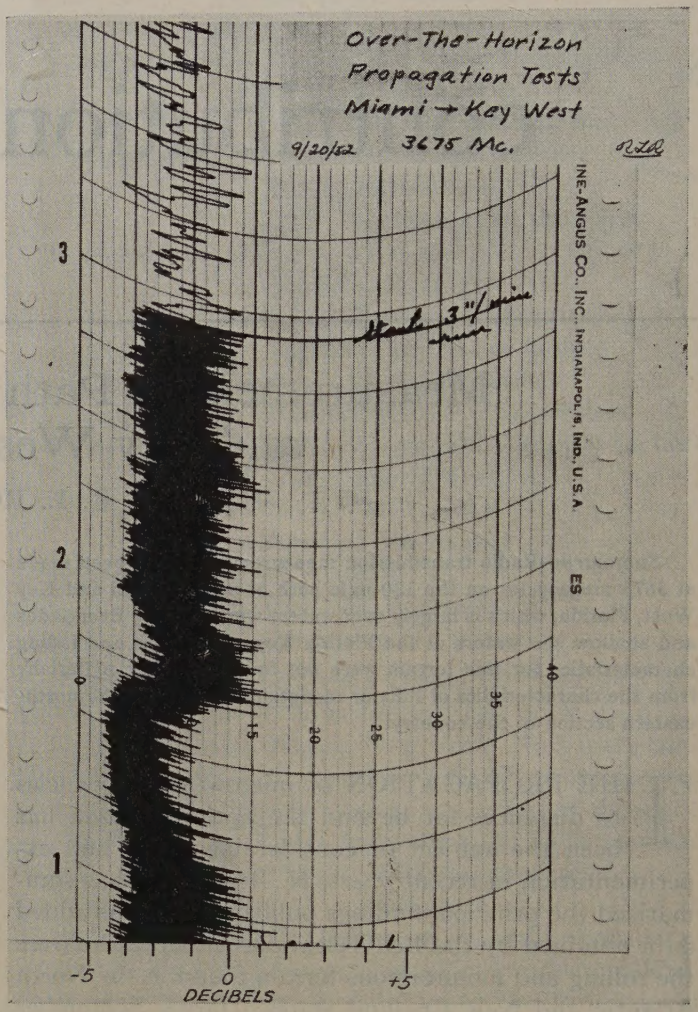

Fig. 2—Typical strip chart recording of received signals.

The curves of Fig. 3 are plots of the data taken by visually averaging, at 15-minute intervals, the recordings made on each of the five transmission paths. Interruptions in the curves are due to equipment failures. There were no signal fade-outs during the period of the tests.

The variation of received signal power with changes of receiving antenna elevation is shown in Fig. 4. The solid line represents data taken by day and the dashed line is for data taken by night. Fig. 5 shows the effect of changing the transmitting antenna elevation. These curves, together with data taken at the "87" Exchange Building and the La Concha Hotel sites, indicate that there is no pronounced advantage to be obtained by elevating the antennas to as much as 100 feet. However, the relatively constant power received with changes of antenna elevation does encourage construction of larger directional antennas.

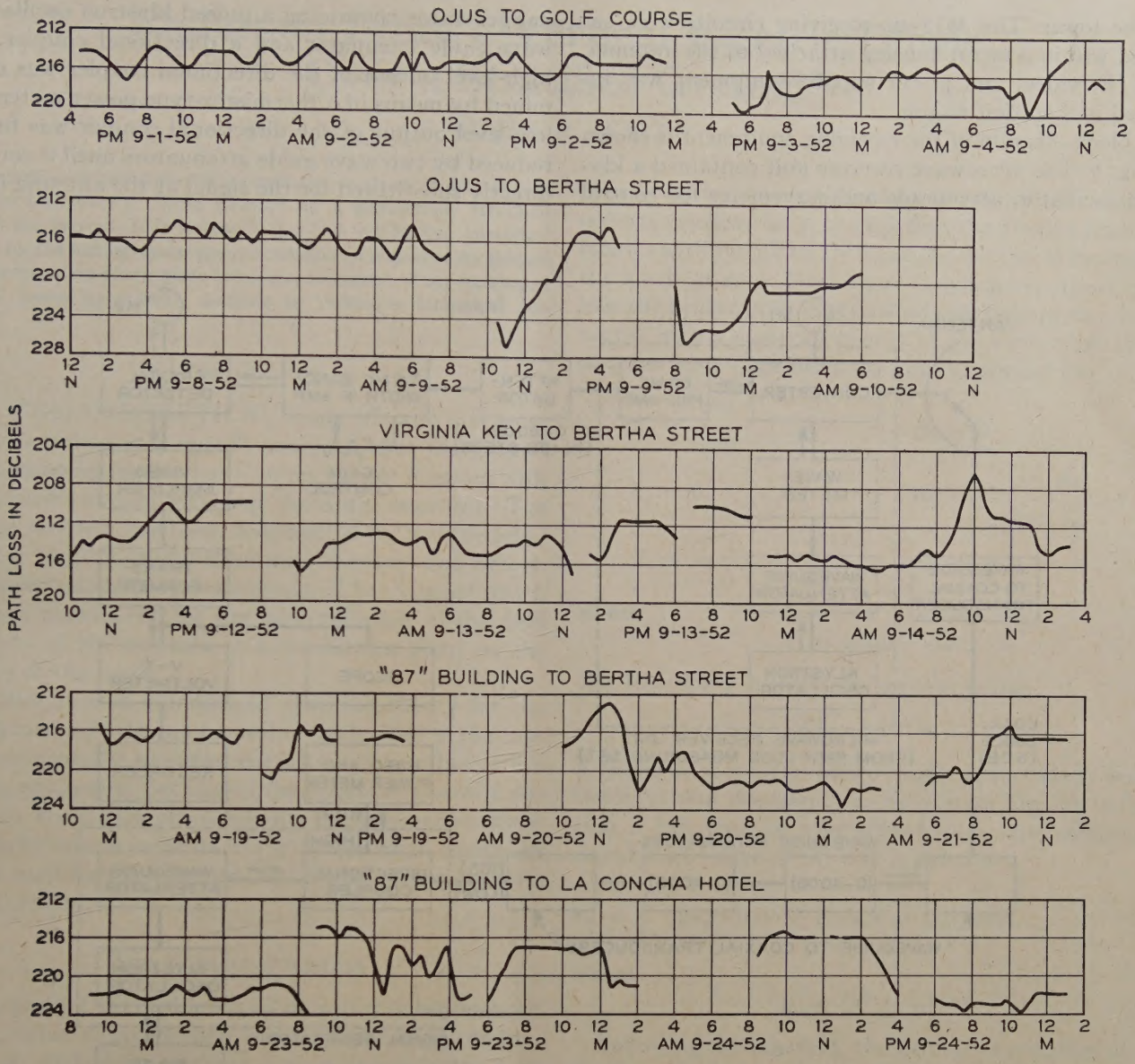

Fig. 3—Measured path losses of five transmission paths tested.

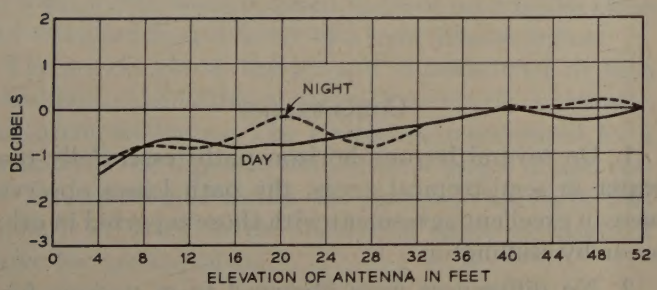

Fig. 4—Variation of received signal power with changes of receiving antenna elevation.

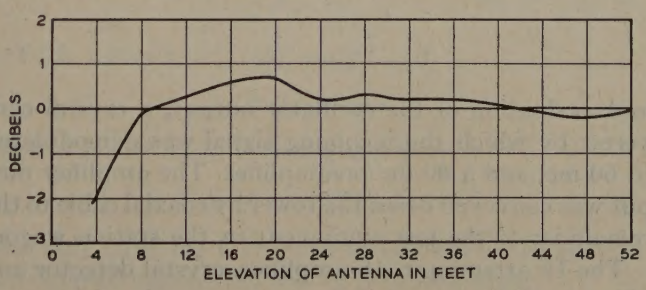

Fig. 5—Variation of received signal power with changes of transmitting antenna elevation.

The test gear comprised two vehicles and the apparatus therein and two transportable steel towers with 57-inch paraboloidal antennas. A conventional radar transmitter of 500-kw peak power and its engine-generator power supply were contained in a $2\frac{1}{2}$-ton truck. The transmitting antenna was fed through wave guide. Each of the antennas was mounted on gimbals so that remotely controlled motors could direct it in azimuth and elevation. In addition, each antenna was supported by a carriage so that it could be elevated to any position

on the tower. The 3675-mc receiving circuits were enclosed within a metal housing attached to the antenna. The IF, video, and power supply equipment was installed in a station wagon.

A block diagram of the receiving equipment is shown in Fig. 6. The microwave receiver unit contained a klystron oscillator, attenuator and wavemeter for control and evaluation of the oscillator output, a crystal converter by which the incoming signal was demodulated to 60 mc, and a 60-mc preamplifier. The amplifier output was conveyed down the tower by coaxial cable to the remainder of the test equipment in the station wagon.

The IF attenuator, IF amplifier, crystal detector and video amplifier provided the necessary gain and control thereof to permit operation and calibration of the vacuum tube voltmeter and its associated recorder. The received pulses were observed on the oscilloscope as previously mentioned. The equipment was calibrated by substituting a pulsed signal of like amplitude, duration and repetition rate, and of known power, for the incoming signal. The calibrating pulse was secured from a signal generator containing a pulsed klystron oscillator, a wave guide attenuator and a directional coupler. The high-level output of the directional coupler was determined by means of a thermistor-type power meter. The low-level output of the directional coupler was further reduced by two wave guide attenuators until it could be directly substituted for the signal at the antenna input

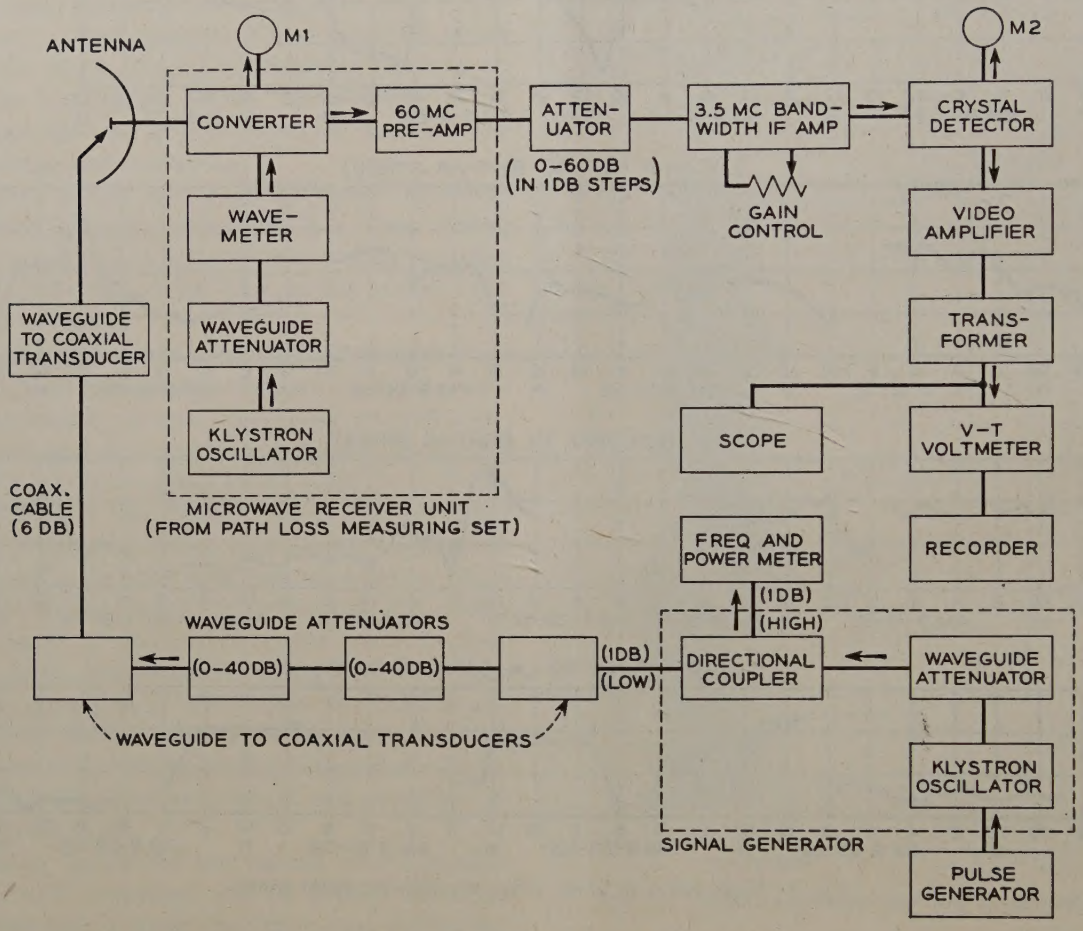

Fig. 6—Block diagram of receiving station equipment.

Conclusions

1. On several beyond-horizon paths essentially over water in semi-tropical areas, the path losses observed were in excellent agreement with those reported in other areas by Bullington.

2. No differences were observed from various foreground terrains. Overland, overwater and well elevated overland take-offs were investigated.

3. Height-loss runs showed uniform received fields over the area that would be occupied by a large high-gain antenna.

4. The diurnal and short-term signal variations were similar to those observed elsewhere.

Radiation From a Vertical Electric Dipole Over a Stratified Ground*

JAMES R. WAIT†

Summary—**Expressions for the radiation fields at low frequencies of a vertical electric dipole situated on a horizontally stratified ground are derived. It is indicated that the well-known numerical results for the homogeneous ground can also be employed for ground wave propagation over a plane conductor composed of any number of parallel layers by suitably defining an "effective numerical distance."**

Introduction

IN THE THEORETICAL study of radiation from an antenna it is usually assumed that the ground may be represented as a homogeneous medium with a specified conductivity and dielectric constant. The general problem has been investigated by Sommerfeld,[1] Van der Pol,[2] Niessen,[3] Bremmer,[4] Norton[5] and others. Extensive charts have been prepared by Norton[5] which are very convenient for the determination of the field intensity of the antenna at some distant point on the surface of the earth.

In this note it is indicated that the theory for the homogeneous earth can be usefully extended to the case of a horizontally stratified earth of any number of homogeneous layers. Because of the approximations in the analysis, the results are valid only for frequencies where the displacement currents in the air are small compared to the combined conduction and displacement currents in the ground.

The Formal Solution

The ground is considered to be suitably represented by a number of layers each with a thickness h, conductivity σ, dielectric constant ϵ, and permeability μ in MKS units. A subscript n is added to these quantities to denote the nth layer from the surface of the ground. The bottom or Nth layer is taken to be of infinite thickness and therefore is equivalent to a semi-infinite region.

The region above the ground is considered to be a semi-infinite insulating space with dielectric constant ϵ_0 and permeability μ_0. The emitter is represented by a vertical electric dipole of infinitesimal length ds and carries a current equal to the real part of I exp. (iωt). The dipole is situated in the insulating space at height h above the ground plane.

It is convenient to introduce a cylindrical polar coordinate system (ρ, ϕ, z) such that the ground plane coincides with the plane $z=0$ and the emitter is located on the z axis at $z=h$. Since there is symmetry about the z axis the fields can be represented everywhere by a Hertz vector with a component only in the z direction and is denoted by π. The fields are then expressed as:

$$E_\rho = \frac{\partial^2 \pi}{\partial \rho \partial z}, \qquad H_\rho = 0,$$

$$E_\phi = 0, \qquad H_\phi = -\frac{\gamma^2}{i\mu\omega}\frac{\partial \pi}{\partial \rho}, \tag{1}$$

$$E_z = -\gamma^2 \pi + \frac{\partial^2}{\partial z^2}\pi, \qquad H_z = 0,$$

where

$$\gamma^2 = i\sigma\mu\omega - \epsilon\mu\omega^2.$$

The function π satisfies the wave equation:

$$(\nabla^2 - \gamma^2)\pi = 0. \tag{2}$$

A subscript n is again added to the quantities to denote the layer that the quantities pertain to. The Hertz function π can then be represented as a superposition of suitable solutions of (2) and is given as:

$$\pi_n = \int_0^\infty [A_n(\lambda)e^{u_n z} + B_n(\lambda)e^{-u_n z}]J_0(\lambda\rho)d\lambda, \tag{3}$$

where

$$u_n = (\lambda^2 + \gamma_n^2)^{1/2}.$$

Following Sommerfeld, the primary excitation of the dipole can be written as follows:

$$\pi_{0p} = ce^{-\gamma_0 r_1}/r_1 = c\int_0^\infty \lambda u_0^{-1} e^{(z-h)u_0} J_0(\lambda\rho)d\lambda, \tag{4}$$

for $z \leqq h$, where $r_1 = [z-h)^2+\rho^2]^{1/2}$ and

$$c = Ids/4\pi i\omega\epsilon.$$

The coefficient $A_0(\lambda)$ is then given by:

$$A_0(\lambda) = e^{-hu_0}\lambda u_0^{-1}.$$

Since only outgoing waves can be allowed in the bottom semi-infinite region (i.e. $n=N$) it is seen that:

$$B_N(\lambda) = 0.$$

The boundary conditions require that the E_ρ and H_ϕ field components are continuous at the interfaces between the layers. These in turn require that the quantities $\partial\pi/\partial_z$ and $\gamma^2\pi$ are continuous at the interfaces. The $2N$ unknown coefficients A_n and B_n can therefore be easily expressed in terms of the known coefficient A_0 by solving the system of $2N$ linear simultaneous equations

* Work carried out under Project No. D48-95-II-14. (After writing this paper the author came upon a paper by J. Grosskopf entitled "Das Strahlungsfeld eines vertikalen Dipolsenders uber geschichtetem Boden," *Hockfreq. u Elek.* 60, pp. 136–141; 1942. Grosskopf obtained a solution for the two layer ground which is a special case of the general result given in this paper.)

† Radio Physics Lab., Defense Research Board, Ottawa, Canada.

[1] A. N. Sommerfeld, *Ann. der Phys.*, vol. 81, p. 1135; 1926.
[2] B. Van der Pol, *Physica*, vol. 2, p. 843; 1935.
[3] K. F. Niessen, *Ann. der Phys.*, vol. 18, p. 893; 1933.
[4] H. Bremmer, *Phil. Mag.*, vol. 25, p. 817; 1938.
[5] K. A. Norton, Proc. IRE, vol. 25, p. 1203; 1937.

derived from the boundary conditions. Omitting the details of the algebra the final result for the Hertz function π_0 in the air is given by:

$$\pi_0 = \pi_{0p} + c\int_0^\infty \lambda u_0^{-1} R(\lambda) e^{-u_0(h+z)} J_0(\lambda\rho) d\lambda, \tag{5}$$

where

$$R(\lambda) = u_0\lambda^{-1}e^{u_0 h}B_0(\lambda) = \frac{K_0 - Z_1}{K_0 + Z_1},$$

$$Z_1 = K_1 \frac{Z_2 + K_1 \tanh u_1 h_1}{K_1 + Z_2 \tanh u_1 h_1},$$

$$Z_2 = K_2 \frac{Z_3 + K_2 \tanh u_2 h_2}{K_2 + Z_3 \tanh u_2 h_2},$$

and so on, until

$$Z_{N-1} = K_{N-1} \frac{K_N + K_{N-1} \tanh u_{N-1} h_{N-1}}{K_{N-1} + K_N \tanh u_{N-1} h_{N-1}}$$

where

$$K_n = u_n(\sigma_n + i\omega\epsilon_n)^{-1}.$$

The formal solution of the problem is thus completely specified. The reduction of this result to a useful form is now undertaken.

The Homogeneous Ground

When the ground is homogeneous such that h_1 tends to infinity, the factor R is simply given by:

$$R(\lambda) = \frac{\gamma_1^2 u_0 - \gamma_0^2 u_1}{\gamma_1^2 u_0 + \gamma_0^2 u_1}.$$

Sommerfeld[1] has shown that for the case of the emitter on the ground, (i.e. $h=0$) that μ_1 can be replaced by γ_1 in the integral if $|\gamma_1^2| \gg |\gamma_0^2|$ so that

$$\pi_0 \cong 2c\int_0^\infty \frac{\lambda e^{-u_0 z} J_0(\lambda\rho) d\lambda}{(\lambda^2 + \gamma_0^2)^{1/2} + \gamma_0^2/\gamma_1}. \tag{6}$$

He also showed that this integral could be expressed in terms of the error function complement with a complex argument for the case $|\gamma_0\rho| \gg 1$ and $z/\rho \ll 1$. His result can be conveniently written as follows:

$$\pi_0 = 2ce^{-\gamma_1 r} r^{-1} F$$

where F is an attenuation factor given by:

$$F = 1 - i(\pi p_1)^{1/2} e^{-p_2} \operatorname{erfc}(ip_2^{1/2})$$

where

$$p_1 = -\frac{\gamma_0^3 \rho}{2\gamma_1^2}$$

and

$$p_2 = p_1\left(1 + \frac{\gamma_1 z}{\gamma_0 \rho}\right)^2.$$

The vertical electric field E_z in the air at the surface of the ground (i.e. $z=0$) with the same approximations, is then given by:

$$E_z = \frac{i\mu\omega I ds e^{-\gamma_0\rho}}{2\pi\rho} F_0 \tag{7}$$

and the horizontal field E_ρ on the surface of the ground is given by:

$$E_\rho = (\gamma_0/\gamma_1) E_z \tag{8}$$

where

$$F_0 = 1 - i\sqrt{\pi p_1}\, e^{-p_1} \operatorname{erfc}(ip_1^{1/2}).$$

The function F_0 has been tabulated by Norton[5] for a range of the values of both magnitude and phase of the complex factor p_1.

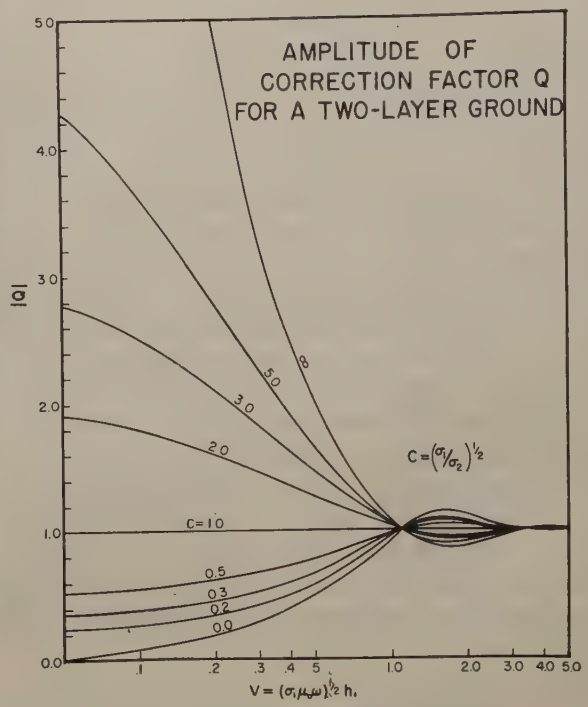

Fig. 1—The amplitude of the wave correction factor Q for a stratified ground composed of two homogeneous layers.

The Stratified Ground

When the ground is stratified such that there are N layers present, the integral expression for π_0 is a great deal more complicated than the corresponding integral for the homogeneous ground discussed in the preceding section. The approximate solution, however, can be obtained in a similar manner by replacing μ_1, μ_2, μ_3, etc. by γ_1, γ_2, γ_3, etc. This will be justified if $|\gamma_1^2/\gamma_0^2|$, $|\gamma_2^2/\gamma_0^2|$, $|\gamma_3^2/\gamma_0^2|$, etc. are much greater than unity. The expression for π_0 for $h=0$, is now given by:

$$\pi_0 \cong 2c\int_0^\infty \frac{\lambda e^{-u_0 z} J_0(\lambda\rho) d\lambda}{(\lambda^2 + \gamma_0^2)^{1/2} + \gamma_0^2/\gamma_e} \tag{9}$$

where γ_e can be called an "effective propagation constant" and is given by:

$$\gamma_e = i\mu\omega/Z_1$$

where

$$Z_1 = \eta_1 \frac{Z_2 + \eta_1 \tanh \gamma_1 h_1}{\eta_1 + Z_2 \tanh \gamma_1 h_1}$$

$$Z_2 = \eta_2 \frac{Z_3 + \eta_2 \tanh \gamma_2 h_2}{\eta_2 + Z_3 \tanh \gamma_2 h_2}$$

and so on, until

$$Z_{N-1} = \eta_{N-1} \frac{\eta_N + \eta_{N-1} \tanh \gamma_{N-1} h_{N-1}}{\eta_{N-1} + \eta_N \tanh \gamma_{N-1} h_{N-1}}$$

where

$$\eta_n = i\mu\omega/\gamma_n.$$

By complete analogy to the case of the homogeneous ground, the electric fields E_z and E_ρ in the air at $z=0$ for $|\gamma_0\rho| \gg 1$ are given by:

$$E_z = \frac{i\mu\omega I ds e^{-\gamma_0\rho}}{2\pi\rho} F_e \tag{10}$$

and

$$E_\rho = (\gamma_0/\gamma_e) E_z \tag{11}$$

where

$$F_e = 1 - i(\pi p_e)^{1/2} e^{-p_e} \operatorname{erfc} (ip_e^{1/2})$$

and

$$p_e = -\frac{\gamma_0^2 \rho}{2\gamma_e^2}.$$

The factor p_e can be called the "effective numerical distance."

The "wave tilt" W is usually defined as the complex ratio of the horizontal field E_ρ to the vertical field E_z, and it is conveniently written:

$$W = W_0 Q$$

where W_0 is the wave tilt for the homogeneous ground given by:

$$W_0 = \gamma_0/\gamma_1$$

and Q is a correction factor given by:

$$Q = \gamma_1/\gamma_e.$$

The "effective numerical distance" p_e can then be written in terms of the numerical distance p_1 for the homogeneous ground as follows:

$$p_e = p_1 Q^2.$$

It can be seen that when $|\gamma_1 h_1| \gg 1$ the factor Q approaches unity and the ground behaves as a homogeneous half-space with electrical constants σ_1, ϵ_1, and μ.

The "Wave Tilt Correction Factor" for a two layer ground (i.e. $h_2 = \infty$) takes the following form:

$$Q = |Q| e^{iq} = \frac{\gamma_1 + \gamma_2 \tanh \gamma_1 h_1}{\gamma_2 + \gamma_1 \tanh \gamma_1 h_1}.$$

When displacement currents in the ground are negligible compared to the conduction currents, such that $\sigma_1 \gg \epsilon_1\omega$ and $\sigma_2 \gg \epsilon_2\omega$ then

$$\gamma_1 \approx i\sigma_1\mu\omega \quad \text{and} \quad \gamma_2 \approx i\sigma_2\mu\omega.$$

The amplitude factor $|Q|$ and the phase q are then plotted in Figs. 1 and 2 as a function of the "relative depth" V, given by $V = (\sigma_1\mu\omega)^{1/2} h_1$ for various values of the conductivity ratio σ_2/σ_1. It is interesting to note that when $V<1$ and $\sigma_2 > \sigma_1$ that the "effective propagation constant" γ_e is somewhat greater than the propagation constant γ_1, of the upper layer. The "effective numerical distance" p_e is also somewhat less than the corresponding value p_1 for the homogeneous ground. At large "numerical distances" such that p_e and p_1 are greater than about ten, a simple expression is obtained for the attenuation factor by considering only the first term of the asymptotic expansion of the error function complement, so that:

$$F_1 \cong -1/2p_1 \quad \text{and} \quad F_e \cong -1/2p_e$$

and then

$$F_e \cong F_1/Q^2.$$

This implies that for this case the field intensity of the ground wave is considerably greater for the stratified ground than for the homogeneous ground.

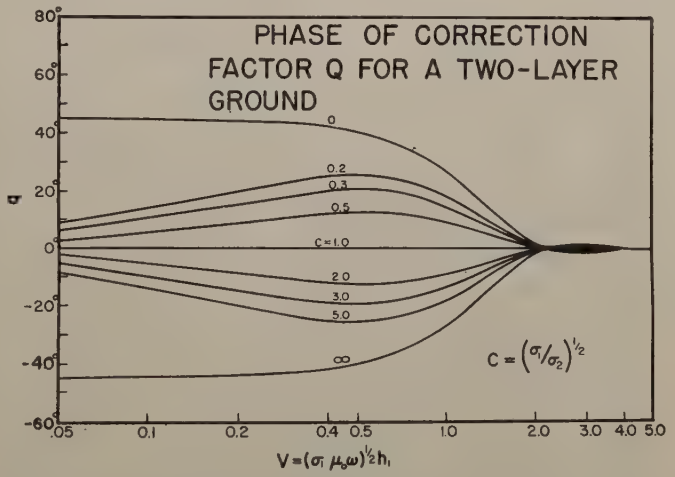

Fig. 2—The phase of the correction factor Q.

For deeper strata such that $V>1$ and $\sigma_2 > \sigma_1$ the field intensity is less for the stratified ground than for the homogeneous ground. For V greater than about 3.0 the factor Q becomes very close to unity, and the field intensity of the ground wave is determined only by the electrical constants of the upper layer. For a frequency of 125 kilocycles per second with a conductivity σ_1, of the upper layer equal to 10^{-2} mhos per meter, the depth h, corresponding to $V=3.0$, is about 30 meters.

It is then concluded that the propagation of the ground wave of a radio-frequency transmitter is not usually influenced by irregularities in the earth's crust, at depths greater than one hundred feet. A similar conclusion was arrived at in a previous paper[6] where a two-dimensional incident wave was considered.

ACKNOWLEDGMENT

Valuable assistance was received from Mr. J. E. Mousseau in performing the necessary calculations.

[6] J. R. Wait, "Geophysics," (in press); April, 1953.

A Two-Dimensional Microwave Luneberg Lens

G. D. M. PEELER†, MEMBER, IRE, AND D. H. ARCHER†

Summary—A two-dimensional microwave model of the Luneberg lens has been designed employing the TE_{10} mode. It consists of two 36-inch diameter, almost-parallel, conducting plates with the space between plates filled with polystyrene. Its thickness varies with the normalized radius, r, to give the desired index of refraction $n=\sqrt{2-r^2}$. Due to symmetry about the center, this lens maintains constant gain and beam shape as a feed is scanned over its circumference, while the side lobe level remains at least 18 db below peak power. Experimental patterns show good agreement with computed patterns in the two principal planes.

Introduction

MANY RADAR SYSTEMS require antennas that can scan a radiation beam over wide angles in space. For low scanning rates, the entire antenna assembly can be moved to position the beam in space. As the scanning rate increases, moving the whole structure becomes impractical because of the large mass, and thus other methods must be used. One method widely used for obtaining higher scanning rates involves moving a low-mass feed over the focal surface of an objective which is capable of maintaining good beam characteristics for various feed positions. The problem, then, is to obtain such an objective.

The parabolic reflector, standard objective for nonscanning antennas, is geometrically perfect when fed at its focus and performs well within a few beamwidths of its axis; but its performance deteriorates rapidly for wider angles.[1] The spherical reflector, although not a perfect objective for any feed position, possesses more symmetry and can be used over wider angles when considered with correctors such as the Schmidt correcting plate[2] or concentric-type correcting elements. The Luneberg lens is an objective possessing complete symmetry. This lens is a sphere of unit radius whose index of refraction n varies with the radius r according to the relation $n=\sqrt{2-r^2}$ as developed by Luneberg.[3] When fed by a source at a point on the surface of the sphere, this lens will focus a beam of rays at infinity (i.e., produce a plane wavefront). Since the focal surface of the lens is the surface of the sphere, the motion of a feed over the surface will produce a corresponding motion of the radiated beam in space without beam deterioration.

This Luneberg sphere, used as a microwave lens together with a suitable feed system, would in many respects be an ideal antenna for complex scans. However, such a three-dimensional lens cannot be easily constructed at this time since there are no suitable materials which will give the needed variation of index of refraction, although some of the expanded dielectrics and artificial dielectrics look encouraging.

For many applications, it is not necessary that the antenna be capable of rapid scanning over a solid angle. An antenna capable of rapid scanning in a plane is quite often desirable, especially if the scan angle is large. This report is concerned with the development of an antenna to meet the latter need.

Several models of the Luneberg lens which scan in a plane have been designed using parallel plate techniques. Rinehart[4] calculated a geodesic analogue which employs the TEM mode in a "derby-hat" shaped parallel-plate region. Experimental models using Rinehart's design have been reported by Fine[5] at the Air Force Cambridge Research Center and by Kunz *et al.*[6] Warren and Pinnell[7] have designed the "tin hat," a variation of the derby-hat which includes a bend in the mean surface near the edge of the lens. Jones[8] designed a model which used the TE_{10} mode in air-filled, almost-parallel plates in which the index of refraction varied with the radius as $n=n_0\sqrt{2-r^2}$, where $n_0<1$. Refraction at the lens aperture ($n_0\neq 1$) was corrected by adding to the edge of the lens a parallel-plate region terminated in a linear aperture. This addition maintains symmetry about only the diameter rather than the center, resulting in beam deterioration and loss of gain off-axis. Jasik[9] of Airborne Instruments Laboratory has designed a spherical Luneberg lens.

Lens Design

The Luneberg lens reported here was designed by using the technique of parallel plates propagating the TE_{10} mode. It was developed in an attempt to eliminate some of the problems encountered in the above-mentioned designs. In order to explain its design, let us begin by considering a dielectric-filled rectangular waveguide. If

† Naval Research Laboratory, Washington, D. C.

[1] K. S. Kelleher and H. P. Coleman, "Off-Axis Characteristics of the Paraboloidal Reflector," NRL Report 4088 (Unclassified); Dec. 31, 1952.

[2] H. N. Chait, "A Microwave Schmidt System," NRL Report 3989 (Unclassified); May 14, 1952.

[3] R. K. Luneberg, "Mathematical Theory of Optics," Brown Univ. Graduate School, Providence, R. I.; 1944.

[4] R. F. Rinehart, "A solution of the problem of rapid scanning for radar antennae," *Jour. Appl. Phys.*, vol. 19, p. 860; 1948.

[5] E. C. Fine, "The Metal-Plate Analogue of a Luneberg Lens," p. 30 of "Proceedings of the Third Symposium on Scanning Antennas," Naval Research Laboratory; November 29–30, 1950.

[6] K. S. Kunz, F. E. Brammer, and J. D. Johannesen, "Final Report on Contract W28-099-ac-141," Case Institute of Technology; September 30, 1949.

[7] F. G. R. Warren and S. E. A. Pinnell, "The Tin Hat Scanning Antenna," and "The Mathematics of the Tin Hat Scanning Antenna," RCA Victor Co. Ltd., Montreal, Canada, Technical Reports 6 and 7; July 16 and Sept. 28, 1951.

[8] S. S. D. Jones, "A Wide-angle Microwave Radiator," *Proc. IEE*, Part III, vol. 97, p. 255; July, 1950.

[9] H. Jasik, "Spherical Luneberg Lens," p. 89 of "Proceedings of the Fourth Symposium on Scanning Antennas," NRL Report 4000; July 18, 1952.

this waveguide is propagating only the TE_{10} mode, the index of refraction is

$$n = \frac{\lambda}{\lambda_g} = \sqrt{\epsilon' - \left(\frac{\lambda}{2a}\right)^2}, \qquad (1)$$

where λ = free-space wavelength; λ_g = waveguide wavelength; a = H-plane dimension of the waveguide; and ϵ' = relative dielectric constant. Since n does not depend on the E-plane dimension of the waveguide, the waveguide may be replaced by a pair of parallel plates.

In this design the plate spacing is varied with position in order to achieve the proper variation of n. The assumption is made that this slight deformation from parallelism has an insignificant effect on the wave velocity at any point, i.e., the index of refraction at a given point depends only upon the spacing at that point. This technique is not truly rigorous since the actual configuration of the plates should be considered as a boundary value problem, the solution probably being expressed as a sum of waveguide modes. The assumption being made is that the magnitudes of modes other than the TE_{10} are small enough to be neglected in this discussion. The concept is not new, for somewhat the same assumption is made in deriving the various modes in a waveguide with walls of finite conductivity.

By combining (1) with the desired index of refraction for a Luneberg lens, $n = \sqrt{2 - r^2}$, the resulting plate spacing is given by

$$a = \frac{\lambda}{2\sqrt{\epsilon' - 2 + r^2}}. \qquad (2)$$

This relation can be readily used to determine the place spacing for experimental models after the wavelength and the dielectric are selected. Examination shows that for $r = 0$, (2) is meaningless unless $\epsilon' > 2$. Other limits on the dielectric constant may be found by specifying operation above cutoff for the TE_{10} mode and below cutoff for higher order TE modes. For operation above cutoff in the TE_{10} mode, let $\lambda < 2a\sqrt{\epsilon'}$ in (2) for $r = 1$ (where cutoff will first occur) and obtain $1 < \sqrt{\epsilon'/(\epsilon' - 1)}$ or $\epsilon' > 1$, which imposes no additional restriction on ϵ'. For operation below cutoff in the TE_{20} mode, let $\lambda > a\sqrt{\epsilon'}$ in (2) for $r = 0$ (the point of greatest difficulty) and obtain $2 > \sqrt{\epsilon'/(\epsilon' - 2)}$, which is satisfied if $\epsilon' > 2.67$.

For our experimental model, designed for a wavelength of 3.2 cm, polystyrene was picked as the dielectric because it was readily available in large slabs, even though its tabulated dielectric constant of 2.48 was less than the minimum of 2.67 specified for operation below cutoff for the TE_{20} mode. It was assumed that there was little possibility of exciting the TE_{20} mode and that it could propagate only in a small region in the center of the lens even if it were excited. Equation (2) was used for determining the plate spacing as a function of the radius. This model, together with a sketch of the cross section which greatly exaggerates the curvature of the plates, is shown in Fig. 1. An aluminum plate was used

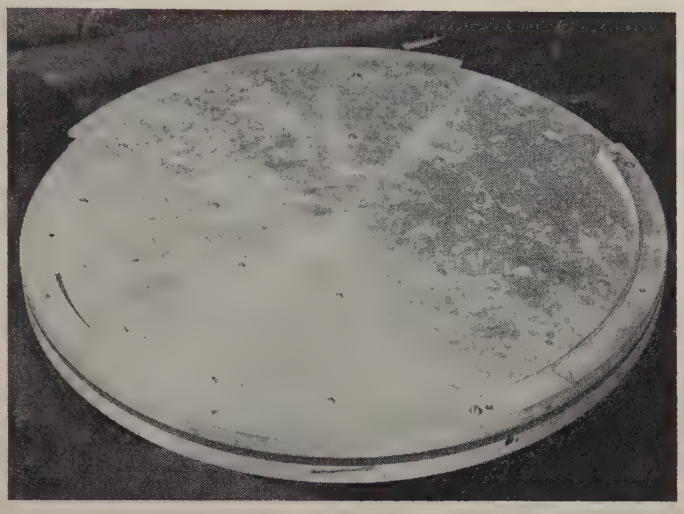

(a)

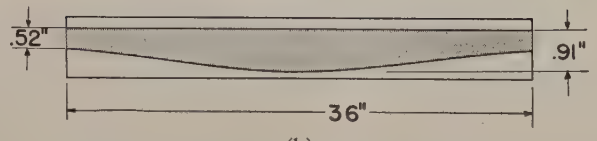

(b)

Fig. 1—Photograph (*a*) and cross-sectional sketch of lens (*b*).

on each side of the polystyrene, the thickness of the upper and lower plates at the circumference being 0.38 and 0.92 inches, respectively. The polystyrene slab was obtained by cementing together two pieces $1 \times 18 \times 36$ inches with Monsanto polystyrene cement #106. The polystyrene seam forms a diameter of the lens.

For ease of construction one surface of the polystyrene was kept plane while the other was machined to the desired contour. With this method of construction the mean surface of the lens is no longer a plane and could cause phase distortion, but the deviation from a plane is slight. The diameter of 36 inches was picked as the largest convenient for obtaining and machining both the aluminum plates and the polystyrene. This choice gives a diameter-to-wavelength ratio of 28.6 which is large enough to produce a reasonable beamwidth. Flanges for positioning a feed were arbitrarily made to cover 90 degrees of the circumference and are located at the rear of the lens. The half-ring at the front of the lens was added to the upper plate so that the dielectric was symmetrically located, making the total thickness 2.36 inches. A small amount of preliminary data indicated improper plate spacing due to a slight warp in the polystyrene slab which occurred after machining. To provide better control of plate spacing bolts were added a few at a time until the data showed that the warping was corrected. These bolts are perpendicular to the electric field and cause negligible reflections.

Lens Illumination

The feed for this lens is shown in Fig. 2. The a-dimension of the waveguide aperture (0.52 inches) was chosen to fit the edge of the lens, and the b-dimension to provide a desirable lens illumination. The waveguide

aperture was filled with polystyrene to permit operation above cutoff. Both the waveguide and the polystyrene were tapered for impedance considerations, the length of the tapers being chosen to keep the variation of waveguide wavelength as small as possible in this transition region. The two metal fins were added in the aperture to suppress the TE_{01} mode which would excite the TEM mode in the lens. The free-space E-plane radiation pattern for this feed is shown in Fig. 3. Cross polarization (presence of the TE_{01} mode) is at least 25 db below peak.

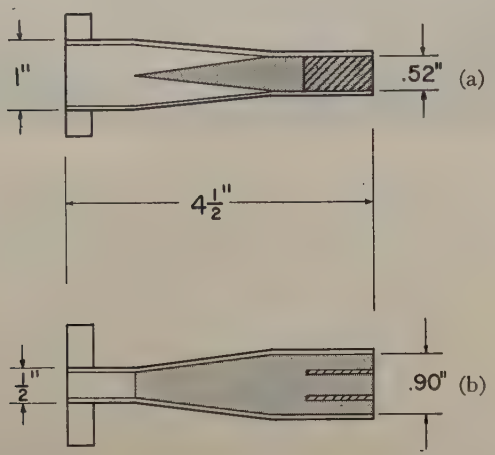

Fig. 2—Feed horn for lens.

A relationship must be found between the distribution of the field from this feed and the field at the lens aperture in order to determine the illumination function at the aperture which will be used later in radiation pattern calculations. This can be done by first considering a typical ray in the lens as shown in Fig. 4. The point P_1 is defined as the point on the ray nearest the origin, O. Due to the symmetry of the lens, the path of the ray is symmetrical about P_1 so that the "triangles" OP_0P_1 and OP_2P_1 are congruent, and $\beta=\gamma$. Since the ray at P_2 is parallel to OP_3, $\gamma=\psi=\beta$.

Energy flow through the lens must now be considered.[10] From principles of geometrical optics it can be shown that energy flow is along rays, and if a tube of rays is considered, that the energy flow is constant through various cross sections normal to the tube. Then the energy flow through the wedge-shaped tube at the feed between β and $\beta+d\beta$ and between x and $x+dx$ is $S_1(\beta, x)d\beta\, dx$, where $S_1(\beta, x)$ is the energy distribution per unit angle in the primary pattern of the feed, and x is the co-ordinate perpendicular to the plane of the lens.

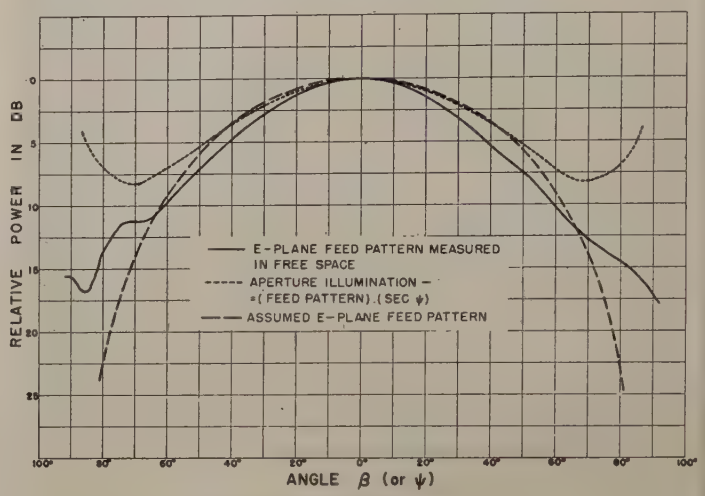

Fig. 3—Feed pattern and aperture illumination.

At the lens aperture in the region of P_2 the energy flow through the tube is $S_a\, dy\, dx$, where S_a is the energy flow per unit area at the aperture. Since S_a is the magnitude of the Poynting vector at the aperture, it will be assumed that it is proportional to the square of the magnitude of the electric field E_a at the aperture. In Fig. 4 it is seen that $y=r_0 \sin \psi$. Then, equating these two energy flows (remembering that $\beta=\psi$), the relation between the aperture field and the feed pattern is

$$|E_a| = C_1\sqrt{S_1 \sec \psi}, \tag{3}$$

where C_1 combines the multiplying constants. This aperture field is also plotted in Fig. 3.

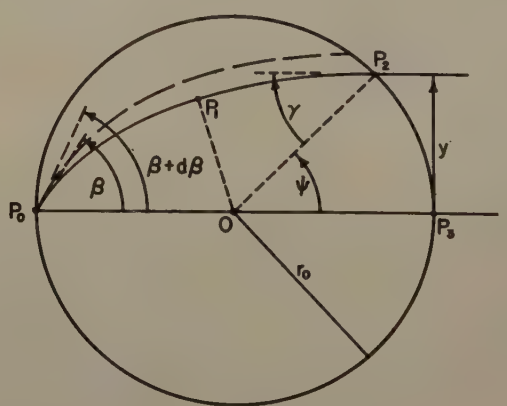

Fig. 4—Typical ray in lens.

[10] The background for these considerations is discussed more fully in Silver, S., ed., "Microwave Antenna Theory and Design," Radiation Laboratory Series, vol. 12, sec. 4.4, McGraw-Hill Book Co., Inc., New York, N. Y.; 1949.

The problem of approximating S_1 with a function that lends itself to mathematical calculation will now be considered. It will be assumed that S_1 is a separable function of x and ψ of the form

$$S_1(y, \psi) = S_2(x) \cdot S_3(\psi). \tag{4}$$

Since the lens employs the TE_{10} mode, $S_2(x)$ is known to be

$$S_2(x) = C_2 \cos^2 \frac{\pi x}{t}, \tag{5}$$

where t is the spacing between plates at the lens aperture and C_2 is a constant. An expression for $S_3(\psi)$ will be chosen to fit the feed pattern as closely as possible. As shown in Fig. 3, if

$$S_3(\psi) = \cos^3 \psi \tag{6}$$

this function fits the feed pattern quite closely for most values of ψ. It was not felt advisable to obtain a closer fit at the wider angles, since there is some doubt as to the exact value of the lens illumination in the region affected by this low-intensity field. The reason for questioning the illumination in this region can be understood by considering the second curve of Fig. 3, which represents the feed pattern multiplied by the space attenuation factor, sec ψ, obtained from geometrical optics. Apparently geometrical optics is not valid in this region. It is felt that the field does not accumulate at the lens edges and then drop sharply to zero, but that some of the energy predicted to appear at the edge of the lens actually appears outside the lens. Therefore, it is felt that the $\cos^3 \psi$ approximation to the pattern is sufficiently accurate. By substituting (4) through (6) into (3) and dropping constant multiplying factors,

$$|E_a| = \cos \frac{\pi x}{t} \cos \psi. \tag{7}$$

Radiation Pattern Calculations

Several of the Luneberg lens reports have considered the problem of calculating the radiation pattern. Warren and Pinnell[7] obtained patterns by numerical integration. Although Walsh[11] avoided numerical integration in a similar problem on cylindrical arrays by approximating the array of discrete elements with a continuous current sheet, it was felt that the Luneberg patterns could be obtained in an easier, more direct manner.

Since rays emerging from the lens are not perpendicular to the aperture, and consequently the field vectors are not parallel to the aperture, it is necessary to consider an approach using these fields for formulating expressions for the radiated field rather than using standard equations containing only scalar functions. The details of these considerations and the calculations (see the Appendix) result in the following expressions for the normalized patterns:

[11] J. E. Walsh, "Radiation patterns of arrays on a reflecting cylinder," Proc. I.R.E., vol. 39, p. 1074; 1951.

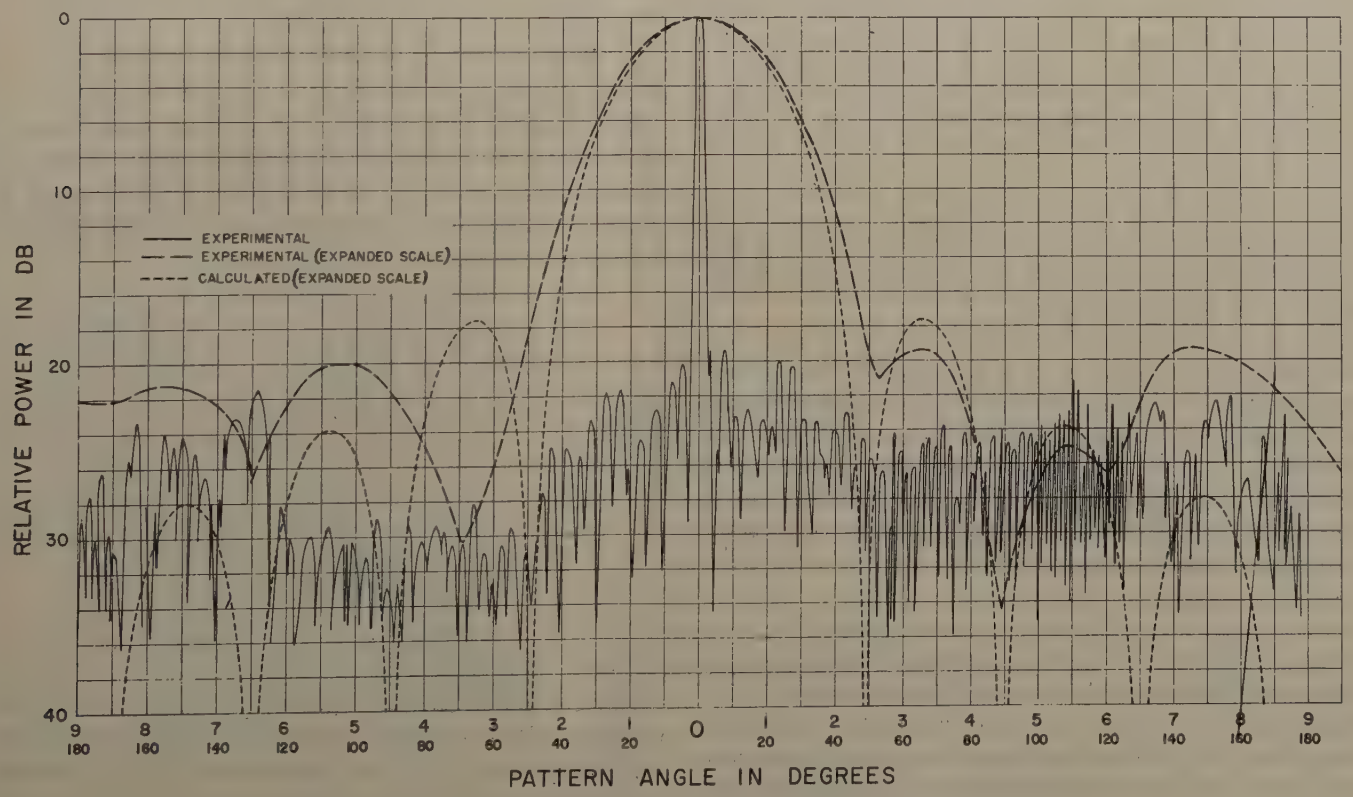

Fig. 5—E-plane calculated and typical experimental radiation patterns.

For the E-Plane:

$$E_\theta(\theta) = \cos^2\frac{\theta}{2}\left[J_0(B) + J_2(B)\right] - j\frac{2\sin\theta}{\pi B^2} \cdot \left[\sin\left(B\cos\frac{\theta}{2}\right) - B\cos\frac{\theta}{2}\cos\left(B\cos\frac{\theta}{2}\right)\right], \quad (8)$$

where $B = 2kr_0 \sin(\theta/2)$, $k = 2\pi/\lambda$ and r_0 = lens radius.

For the H-Plane:

$$E_\phi(\theta) = \left[\frac{\left(\frac{1+\cos\theta}{2}\right)\cos\left(\frac{kt\sin\theta}{2}\right)}{1-\left(\frac{kt\sin\theta}{\pi}\right)^2}\right] \cdot \left[\left\{J_0(D) = \frac{J_1(D)}{D}\right\} - j\left\{H_0(D) - \frac{H_1(D)}{D}\right\}\right], \quad (9)$$

where $D = 2kr_0 \sin^2(\theta/2)$ and t = aperture height.

These radiation patterns, given above by (8) and (9), are plotted in Figs. 5 and 6, where they can be compared with experimental patterns.

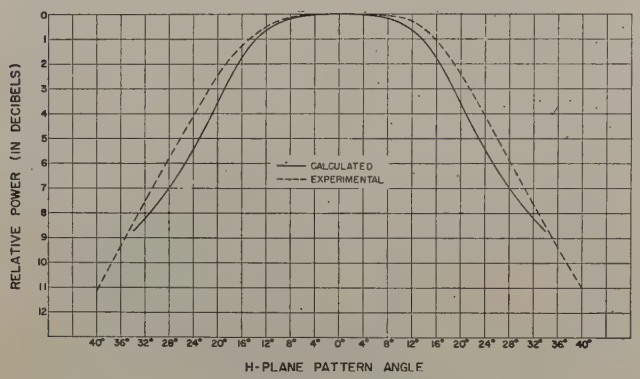

Fig. 6—H-plane calculated and typical experimental radiation patterns.

Beamwidth Formulas

The preceding solutions of the radiation field will now be used to develop formulas for the half-power beamwidths of the Luneberg lens.

The E-plane radiation pattern given in (8) is rather unwieldy for this purpose, but considerable simplification occurs if the range of values which r_0/λ may assume is restricted. Calculation has shown that for $r_0/\lambda \geqq 7$ the effect of the second term in this equation is completely negligible and $\cos^2(\theta/2)$ may be replaced by unity. Therefore, with r_0/λ sufficiently large, the expression for the radiation pattern becomes

$$E(\theta) = J_0(B) + J_2(B) = f(B).$$

A plot of $E(\theta)$ versus B gives a universal radiation pattern valid for a lens of any size. From this pattern the beamwidth can be expressed in terms of B or r_0/λ. However, this same information can be obtained from the plot of (8) for the experimental lens by noting that the half-power points occur at angles $\theta_1 = \pm 1.03°$. Thus, for any lens, $\theta_1 = 2\sin^{-1}(B_1/2kr_0)$, and the full beamwidth is given by

$$\Theta_E \approx 29.4\left(\frac{\lambda}{r_0}\right) \quad (10)$$

in degrees. This equation is plotted in Fig. 7.

Calculation has shown that for $7 \leqq r_0/\lambda \leqq 70$ the first term in (9) may be approximated by a constant. Thus the H-plane radiation pattern may be written as $E(\theta) = g(D)$, and a plot of $E(\theta)$ versus D shows that the half-power points occur at angles $\theta_1 = \pm 19°$. Thus, for any lens, $\theta_1 = 2\sin^{-1}\sqrt{D_1/2kr_0}$, and the full beamwidth is given by

$$\Theta_H \approx 143\sqrt{\lambda/r_0} \quad (11)$$

in degrees. This equation is also plotted in Fig. 7.

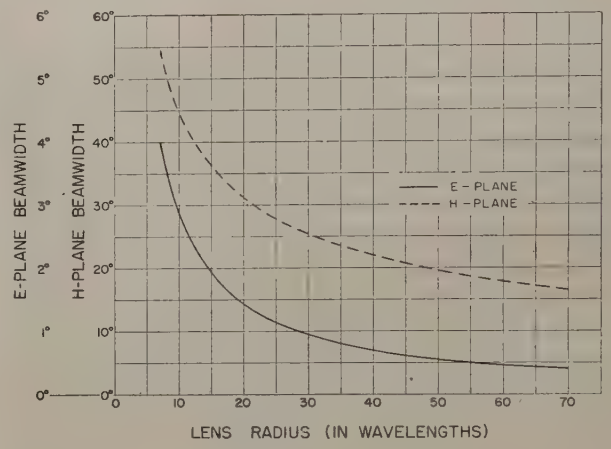

Fig. 7—Beamwidths versus r_0/λ for E- and H-planes.

Experimental Evaluation of the Lens

Phase Measurements

The phase front in the plane of the lens was measured using standard techniques.[12] A typical set of data is shown in Fig. 8. For a range of pickup positions of 25 inches the maximum deviation from a linear phase front is 0.025 wavelengths.

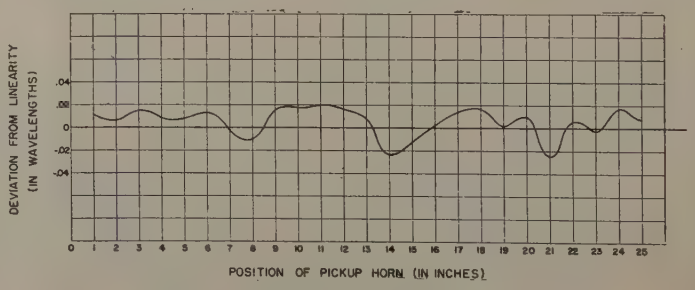

Fig. 8—Typical phase front of lens.

E-Plane Patterns

Early E-plane patterns taken with the lens assembled without bolts had an unsymmetrical beam shape due to the slightly warped polystyrene which caused incorrect

[12] For example, see Silver, S., *op. cit.*, sec. 15.11.

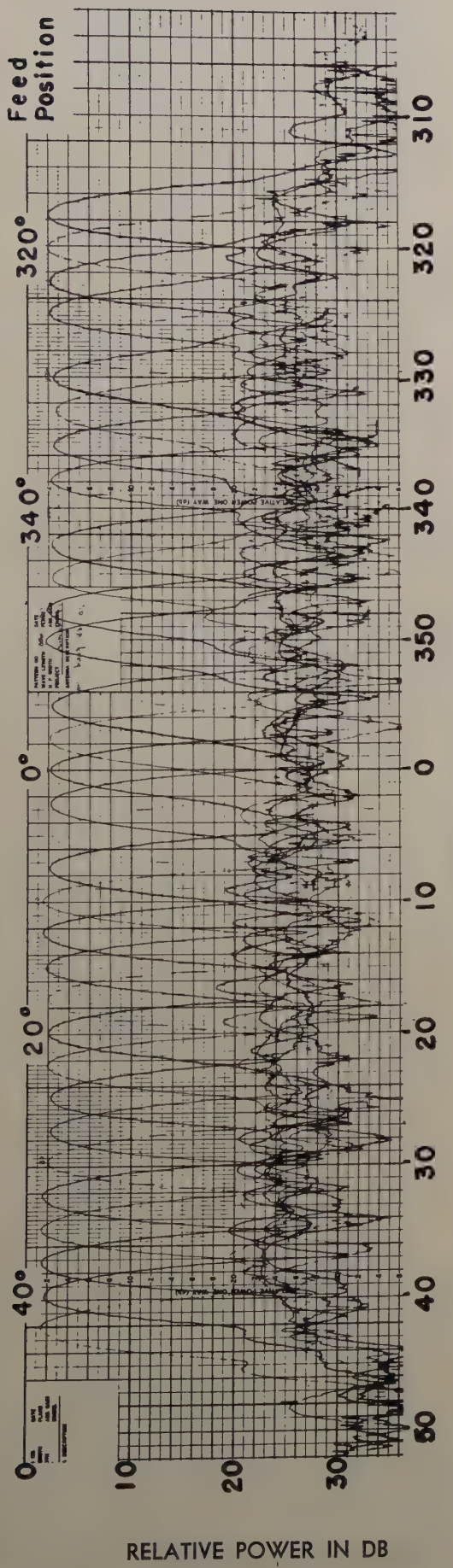

Fig. 9—E-plane radiation patterns for various feed positions.

plate spacing. As mentioned previously, the addition of the bolts corrected this difficulty. Patterns taken with the polystyrene seam in various positions show no appreciable effects due to its presence.

A typical E-plane pattern for the feed at zero degrees shown in Fig. 5 was a half-power beamwidth of 2.2 degrees and side lobes 19.4 db below peak power. The beamwidth factor, defined as (beamwidth×lens diameter)/wavelength, is 63 degrees for this lens, which indicates high efficiency in this plane. This pattern agrees quite well with the calculated pattern, plotted in Fig. 5.

E-plane patterns for feed positions in increments of 2.5 degrees around the circumference of the lens are shown in Fig. 9. Over the 90-degree range permitted by the flanges, the gain and beam shape remain reasonably constant, and most of the side lobes are at least 18 db below peak power. The angle of beam shift is equal to the angle of feed shift.

H-Plane Patterns

Fig. 6 contains plots of a typical H-plane pattern for the feed at zero degrees and the calculated pattern given by (9). These patterns have flat tops and no side lobes or minima as such, but the skirts extend to rather large angles. The half-power beam widths are 42.8 and 38 degrees for the experimental and calculated patterns respectively.

Because of the end-fire effect present in this plane, these beamwidths are much smaller than would be expected from the H-plane aperture of 0.52 inch. This end-fire effect might be seen in the calculated pattern given in (9) if the first bracket is considered as the "element pattern" and the second bracket as the "array factor." The H-plane beamwidth formula given by (11) shows that, due to this end-fire effect, the beamwidth varies inversely as the square root of the lens radius. Therefore, if the lens radius were increased to obtain a smaller E-plane beamwidth, the H-plane beamwidth also becomes smaller; however, for any practical radius the lens produces a fan-shaped beam. If a more directive beam is desired, it is necessary to increase either the H-plane aperture or the aperture efficiency, or both, i.e., by obtaining a more directive "element pattern."

Addition of Flares

In order to increase the lens aperture, the addition of flares was considered, keeping in mind as requirements for the flares: symmetry about the center of the lens, freedom of feed movement, and noninterference with E-plane patterns. Since this lens uses the TE_{10} mode, the addition of any flares makes the index of refraction less than unity within the flares. Since Luneberg's resulting variation of index of refraction inside the lens is based on the lens being imbedded in a medium with an index of unity, the effects of the addition of flares should be compensated for in a redesign of the lens. Although analytical attempts to include flares in a lens design were unsuccessful, the experimental addition of flares proved somewhat fruitful.

Two sets of flares were investigated. A photograph of one set mounted on the lens is shown in Fig. 10. These "conical flares" are composed of plane sections cut to a radius of 20 inches (two inches larger than the lens radius) to which are soldered 7-inch sections of a 90 degree cone, making the total H-plane aperture approximately 12 inches. These flares increase both the aperture size

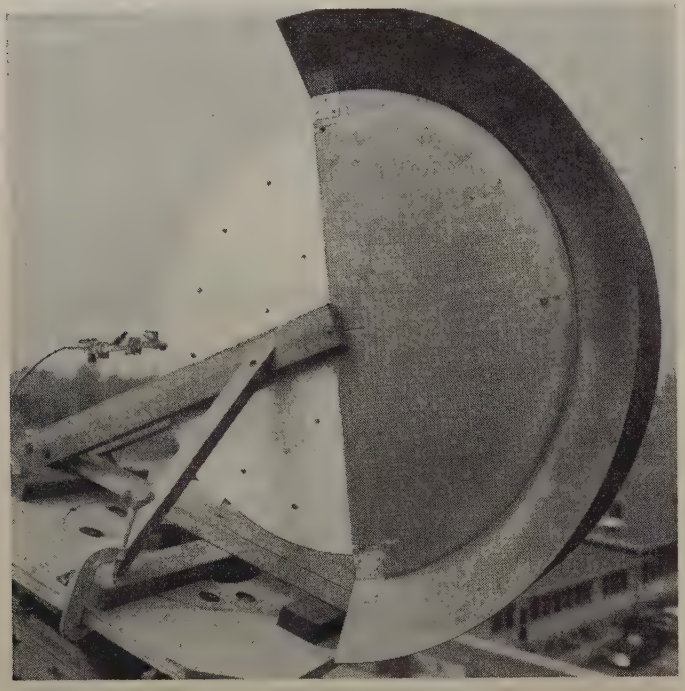

Fig. 10—Lens with conical flares.

and its efficiency, the greater efficiency resulting from the box horn[13] formed by the lens and the plane sections. This conical section could not be extended to the actual aperture of the lens since the spacing between flares would then be small enough to make that region below cutoff. Mounting slots permit adjustment of the flares relative to the lens. An H-plane pattern for the best position of the flares is shown in Fig. 11, where it can be

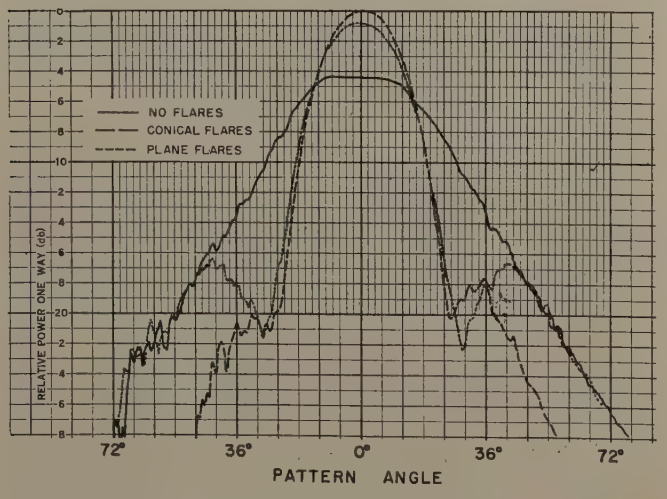

Fig. 11—H-plane radiation patterns for flares in best position.

[13] See Silver, S., *op. cit.*, sec. 10.15.

compared with other patterns. With these flares the half-power beamwidth of this pattern is decreased to 22 degrees and side lobes are 18 db below peak power.

A second set of "plane flares," made identical to the plane sections of the conical flares and which provide an H-plane aperture of 2.36 inches, was also tried. An H-plane pattern with these flares adjusted to the best position is also shown in Fig. 11. The half-power beamwidth of this pattern is 24 degrees, and side lobes are 16 db below peak power.

A comparison of patterns in Fig. 11 shows little difference in the patterns taken with the two sets of flares. The larger aperture of the conical flares obtains little reduction in beamwidth or side lobe level and increases the gain by less than 1 db. It is felt that the smaller size of the plane flares will in most applications make them more useful. In the next section, concerned with stacking these lenses to obtain further reduction in H-plane beamwidth, these smaller flares must be used.

As was pointed out earlier, the addition of flares alters the optics of the lens; however, E-plane patterns taken with the conical flares for various feed positions as shown in Fig. 12 indicate little variation from those in Fig. 9 for the lens without flares.

Since these flares improve the H-plane patterns without appreciable effect on E-plane patterns, they can also be utilized as flanges for positioning the feed. Thus, by extending them over the full circumference of the lens, full 360-degree scanning can be accomplished.

Stacked Lenses

Since the use of flares to sharpen the beam of this lens proved limited, a further reduction in the H-plane beamwidth was obtained by stacking several of these lenses one above the other and feeding them in phase. The stacking of two lenses will now be considered. Let d be the separation between centers of the apertures and θ be the H-plane pattern angle as indicated in the Appendix. Then at the angle θ in the H-plane there is a phase difference of $(2\pi d/\lambda) \sin \theta$ between the fields from the two lenses. If $E(\theta)$ is the field of a single lens, this combination will produce the field

$$E_1(\theta) = E(\theta) + E(\theta)e^{(j2\pi d \sin \theta)/\lambda}$$

$$= 2E(\theta)e^{(j\pi d \sin \theta)/\lambda} \cos \frac{\pi d \sin \theta}{\lambda}.$$

If $E(\theta)$ is approximated by $e^{-c_3\theta^2}$, where c_3 is a constant which is equal to 0.00347 for a single lens beamwidth of 20 degrees, this expression becomes, when considering only the normalized magnitude,

$$E_2(\theta) = e^{-0.00347\theta^2} \cos \frac{\pi d \sin \theta}{\lambda}. \qquad (12)$$

The resulting beamwidth and side-lobe level are thus a function of the separation, d. For any given value of d, the half-power beamwidth is obtained by equating $E_2(\theta)$ to 0.707 and solving the resulting transcendental

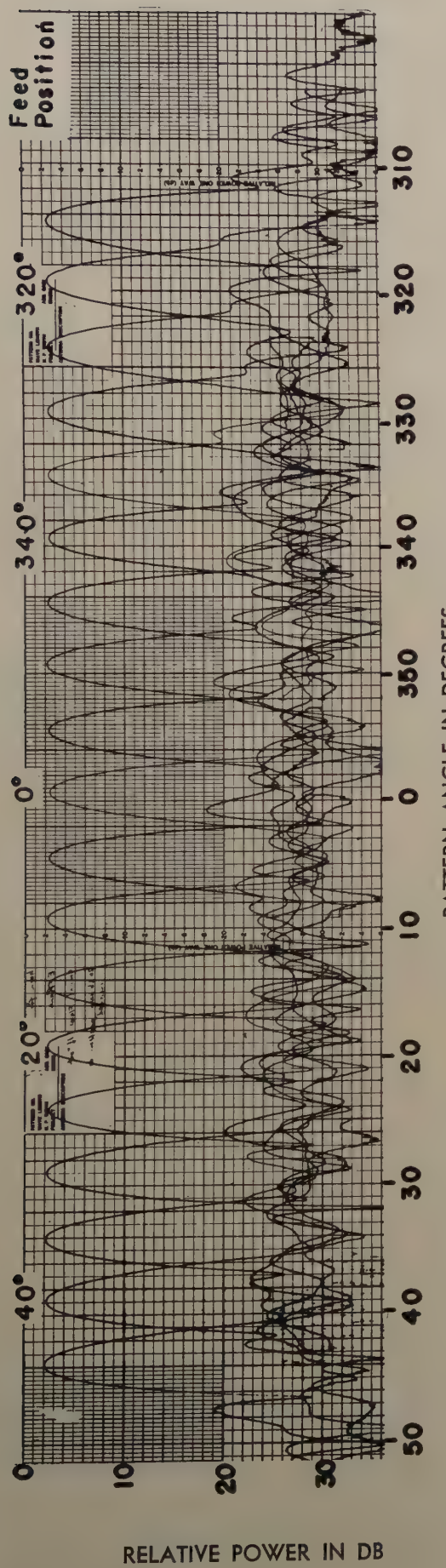

Fig. 12—E-plane radiation patterns for various feed positions with conical flares.

equation for θ_1, the half-beamwidth. The m^{th} side lobe occurs approximately at $\theta = \sin^{-1}(m\lambda/d)$, and its level can be found by substituting this angle in (12). For this double-lens combination, the half-power beamwidth and the first side-lobe level for several values of d are given in Table 1.

TABLE I
H-Plane Half-Power Beamwidth and First Side-Lobe Level for Double-Lens Combination

d	Half-Power Beamwidth (degrees)	First Side-Lobe Level (db)
2λ	11.8	26.9
2.5λ	10.1	16.7
3λ	8.7	11.4

Contour Patterns

Since a phase front from this lens is not a plane, but somewhat saddle-shaped, it is not immediately apparent that the largest side lobes are found in the principal planes. For this reason, other sections through the radiation beam were explored. A contour plot of the beam structure from the lens without flares is shown in Fig. 13. No side lobes appear which are greater than those found in the principal planes. Measurements taken for the lens with flares gave a similar result.

Pattern Bandwidth

All the data presented thus far were taken at a wavelength of 3.2 cm. However, Table 2 gives E-plane pattern characteristics for a range of frequencies from 8,900 mc to 9,800 mc for the lens without flares. Within this 9.6 per cent band the patterns are essentially constant. At lower frequencies, the beam shape begins to deteriorate with an accompanying increase in the side-lobe level. Equipment was not available for taking measurements at higher frequencies. Similar results were obtained for the lens with flares.

TABLE 2
E-Plane Pattern Characteristics for Various Frequencies

Frequency (mc)	Beamwidth (degrees)	Side-Lobe Level (db)	Beamwidth Factor (degrees)
8900	3.1	16.9	88.6
9000	2.8	15.6	80.0
9100	2.5	18.0	71.4
9200	2.3	19.9	65.7
9300	2.25	17.5	64.3
9375	2.25	20.4	64.3
9500	2.2	18.8	62.9
9600	2.3	19.5	65.7
9700	2.4	20.8	68.6
9800	2.6	19.7	74.3

Impedance Match

For the lens without flares, the vswr in the feed line is below 1.4 over most of the range of λ from 3.1 to 3.5 cm. No attempts were made to obtain an impedance match other than putting tapers in the feed as shown in Fig. 2. However, since the characteristic impedance of the lens at its edge is equal to that of free space at the design

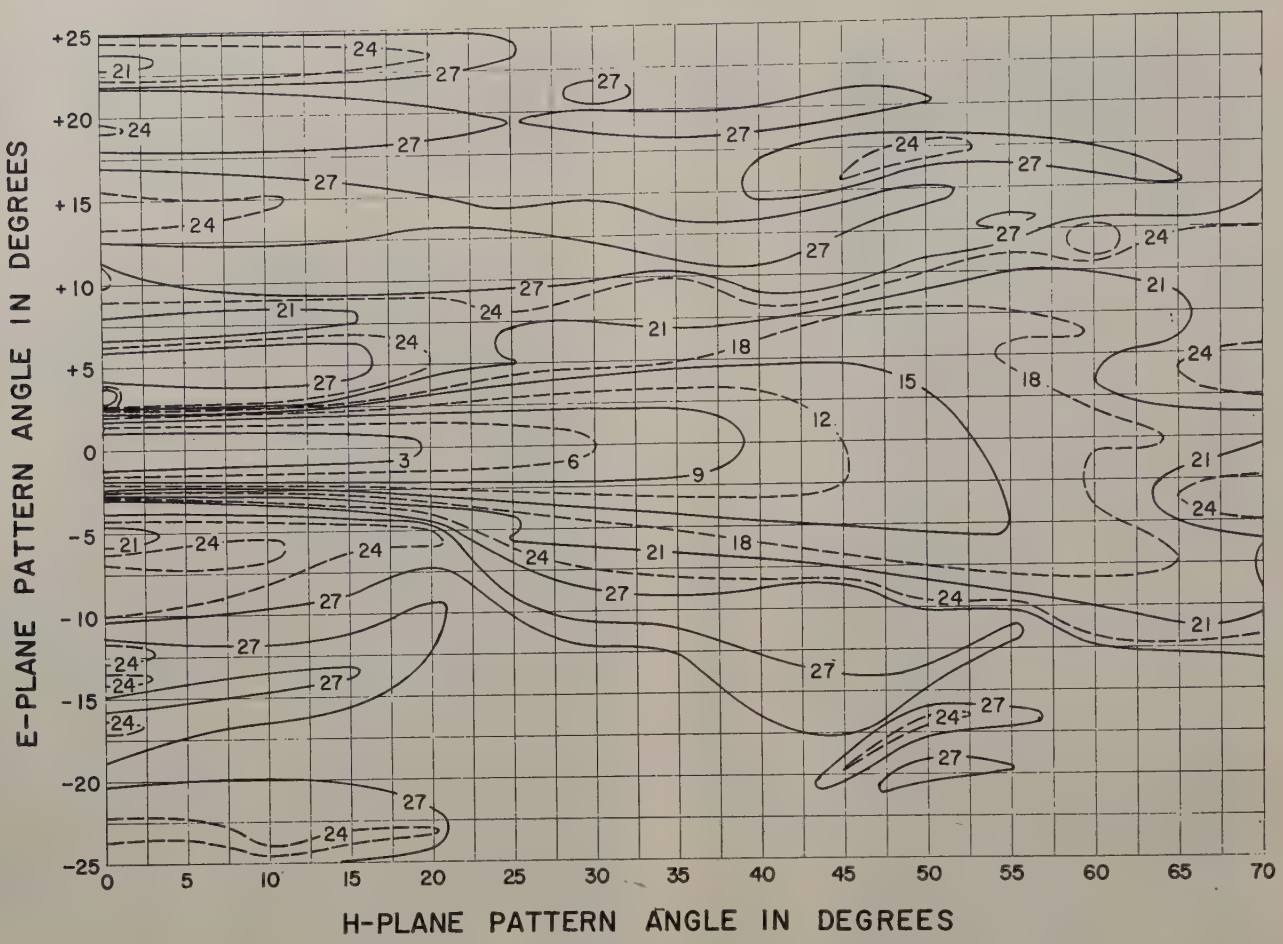

Fig. 13—Radiation pattern contour plot (in 3 db steps) for lens with no flares.

wavelength, the lens possesses an inherent match in this region. Mismatch between feed and lens was not investigated except to decide that no choke is needed at this junction since currents for the TE_{10} mode are parallel to the gap between the plates of the lens and the feed.

Gain

The difference in peak power in the patterns of Fig. 11 gives a comparison between the gain of the lens with and without flares. The measured gain at $\lambda = 3.2$ cm was 22.2 db for the lens only and 25.9 db for the lens with the plane flares.

There are several bases for evaluating the gain from pencil-beam antennas and, although this antenna does not produce a pencil beam, such methods will be used. The first method is to compare the gain with that expected from a uniformly illuminated aperture which is $4\pi A/\lambda^2$, where A is the aperture area. For this lens with the plane flares, the projected aperture is 40×2.36 inches, so that at $\lambda = 3.2$ cm, $4\pi A/\lambda^2 = 750 = 28.8$ db. A comparison of the measured gain of 25.9 db = 389 with this figure shows that the aperture efficiency is 0.52, which is good for a wide-angle scanner.

The second method is to compare the gain with $27{,}000/\theta_E\,\theta_H$, where θ_E and θ_H are the E- and H-plane half-power beamwidths in degrees, respectively. If the beamwidths for this lens with the plane flares are substituted in this expression, it becomes $27{,}000/(2.2 \times 24) = 512 = 27.1$ db. There is a difference of 1.2 db between this figure and the measured gain.

If account is taken of a small loss in the polystyrene of the lens and also the power contained in side lobes which in the E-plane do not fall off rapidly with angle, this lens appears quite efficient.

Conclusions

A two-dimensional microwave analogue of the Luneberg lens which utilizes the TE_{10} mode has been designed which produces good radiation patterns and maintains good pattern characteristics over its limit of scan and over a band of frequencies. The calculated and experimental patterns agree quite well.

This lens design lends itself to easy construction by requiring machining of only one surface of the dielectric, resulting in a lens with a small volume which is quite rugged. The weight of this lens can be reduced to that of the dielectric alone by coating the dielectric with a thin metallic layer and eliminating the heavy aluminum plates and the bolts used in the model described heretofore. The shape of this lens permits the addition of flares and the stacking of several lenses to produce a more directional beam than a single lens possesses. The flares may be used to position the feed, thereby permitting scanning over the full 360 degrees.

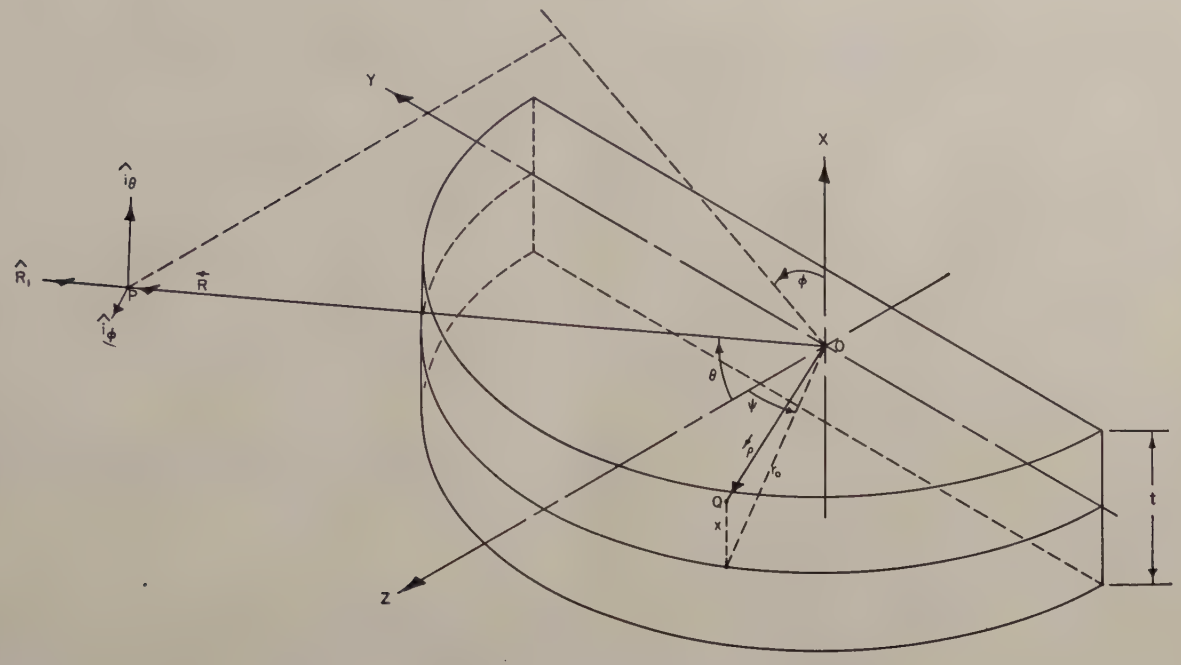

Fig. 14—Co-ordinate systems for radiation pattern calculations.

Acknowledgments

The authors would like to thank K. S. Kelleher of the Washington Branch of the Naval Research Laboratories for his many helpful suggestions during the course of this project, and H. P. Coleman of the same Branch for his assistance in taking radiation patterns and preparing the figures.

Appendix

RADIATION PATTERN CALCULATIONS

The aperture-field method will be used to calculate the far-field radiation pattern of the Luneberg lens. The solution appears in the literature,[14] and the components of the radiation field are

$$E_\theta = -\frac{j\omega\mu_0}{4\pi R} e^{-jkR} \int_S \left[\hat{n}\times\vec{H}_a \cdot \hat{\imath}_\theta - \sqrt{\frac{\epsilon_0}{\mu_0}}\, \hat{n}\times\vec{E}_a \cdot \hat{\imath}_\phi \right] \cdot e^{jk\vec{\rho}\cdot\hat{R}_1} ds, \quad (13)$$

$$E_\phi = -\frac{j\omega\mu_0}{4\pi R} e^{-jkR} \int_S \left[\hat{n}\times\vec{H}_a \cdot \hat{\imath}_\phi + \sqrt{\frac{\epsilon_0}{\mu_0}}\, \hat{n}\times\vec{E}_a \cdot \hat{\imath}_\theta \right] \cdot e^{jk\vec{\rho}\cdot\hat{R}_1} ds, \quad (14)$$

where $\vec{E}_a$ and $\vec{H}_a$ are the values of the field in the aperture and $\hat{n}$ is the outward-drawn unit vector normal to the aperture. Referring to Fig. 14, these expressions may be simplified by the following considerations. Since the lens was designed to produce constant phase in the plane of the lens along the line tangent to the aperture center, $\vec{E}_a$ and $\vec{H}_a$ have a phasing of $kr_0(1-\cos\Psi)$ where $k=2\pi/\lambda$ and r_0 is the lens radius. Let $\vec{E}_a$ be directed along the negative Y-axis since, in the TE_{10} mode, the electric field is perpendicular to the direction of propagation which at the aperture is parallel to the Z-axis. Then it follows that $\vec{H}_a$ must be directed along the positive X-axis. Also, since the lens was designed to give an index of refraction of unity in the aperture, $\vec{E}_a$ and $\vec{H}_a$ are related as in a plane wave. Thus the aperture field may be expressed as

$$\vec{E}_a = -\hat{\imath}_y \left| E_a \right| e^{jkr_0(1-\cos\psi)}, \quad (15)$$

$$\vec{H}_a = \hat{\imath}_x \left| E_a \right| \sqrt{\frac{\epsilon_0}{\mu_0}}\, e^{jkr_0(1-\cos\psi)}. \quad (16)$$

From Fig. 14 it follows that

$$\vec{\rho} = \hat{\imath}_x x - \hat{\imath}_y r_0 \sin\psi + \hat{\imath}_z r_0 \cos\psi, \quad (17)$$

$$R_1 = \hat{\imath}_x \sin\theta\cos\phi + \hat{\imath}_y \sin\theta\sin\phi + \hat{\imath}_z \cos\theta, \quad (18)$$

$$\hat{\imath}_\theta = \hat{\imath}_x \cos\theta\cos\phi + \hat{\imath}_y \cos\theta\sin\phi - \hat{\imath}_z \sin\theta, \quad (19)$$

$$\hat{\imath}_\varphi = -\hat{\imath}_x \sin\phi + \hat{\imath}_y \cos\phi, \quad (20)$$

$$\hat{n} = -\hat{\imath}_y \sin\psi + \hat{\imath}_z \cos\psi. \quad (21)$$

If (15) through (21) are substituted into (13) and (14), they take the form

$$E_\theta = -\frac{j\omega r_0\sqrt{\mu_0\epsilon_0}}{4\pi R} e^{-jkR} \int_s \left| E_a \right| e^{jkR_0(1-\cos\psi)} \cdot \left\{ \cos\psi \sin\phi(\cos\theta + 1) - \sin\psi\sin\theta \right\} e^{jk\vec{\rho}\cdot\hat{R}_1} d\psi dx \quad (22)$$

$$E_\phi = -\frac{j\omega r_0\sqrt{\mu_0\epsilon_0}}{4\pi R} e^{-jkR} \int_s \left| E_a \right| e^{jkr_0(1-\cos\psi)} \cdot \cos\psi\cos\phi(1+\cos\theta) e^{jk\vec{\rho}\cdot\hat{R}_1} d\psi dx. \quad (23)$$

[14] S. Silver, *op. cit.*, p. 161, equation (103).

Substituting (7) for $|E_a|$ into these two equations and dropping constant multiplying factors, they become

$$E_\theta = \int_{-t/2}^{t/2} \cos\frac{\pi x}{t}\,dx \int_{-\pi/2}^{\pi/2} \cos\psi\{\cos\psi\sin\phi(1+\cos\theta) - \sin\psi\sin\theta\}e^{-jkr_0\cos\psi e^{jk\vec{\rho}\cdot\hat{R}_1}}d\psi, \quad (24)$$

and

$$E_\phi = \int_{-t/2}^{t/2} \cos\frac{\pi x}{t}\,dx \int_{-\pi/2}^{\pi/2} \cos^2\psi\cos\phi(1+\cos\theta) \cdot e^{-jkr_0\cos\psi e^{jk\vec{\rho}\cdot\hat{R}_1}}d\psi. \quad (25)$$

Since patterns in the principal planes are of greatest interest, these special cases will now be considered.

E-Plane Pattern

For the E-plane pattern, the far-field point P is confined to the yz-plane where $\phi = \pm 90°$, but due to symmetry about this plane, only one value of ϕ need be considered. Inspection of (17) and (18) for $\phi = -90°$ shows

$$\vec{\rho}\cdot\hat{R}_1 = r_0\sin\psi\sin\theta + r_0\cos\psi\cos\theta = r_0\cos(\psi-\theta).$$

Then (24) and (25) may be written

$$E_\theta(\theta) = \int_{-t/2}^{t/2} \cos\frac{\pi x}{t}\,dx \int_{-\pi/2}^{\pi/2} \cos\psi[\cos(\psi-\theta)+\cos\psi] \cdot e^{jkr_0[\cos(\psi-\theta)-\cos\psi)]}d\psi, \quad (26)$$

$$E_\phi = 0.$$

Since the integral in x in (26) is independent of θ, it is a constant as far as the radiation pattern is concerned, and thus may be neglected. The second integral may be rearranged to give

$$E_\theta(\theta) = \cos\theta/2\int_{-\pi/2}^{\pi/2} \cos\psi\cos(\psi-\theta/2) \cdot e^{2jkr_0\sin\theta/2\sin(\psi-\theta/2)}d\psi. \quad (27)$$

Making the substitutions $B = 2kr_0\sin\theta/2$ and $\alpha = \psi - \theta/2$ gives

$$E_\theta(\theta) = \cos\theta/2\int_{-\pi/2-\theta/2}^{\pi/2-\theta/2} \cos\left(\alpha+\frac{\theta}{2}\right)\cos\alpha e^{jB\sin\alpha}d\alpha,$$

$$E_\theta(\theta) = \cos^2\frac{\theta}{2}\int_{-\pi/2-\theta/2}^{\pi/2-\theta/2} \cos^2\alpha e^{jB\sin\alpha}d\alpha - \frac{\sin\theta}{2}\int_{-\pi/2-\theta/2}^{\pi/2-\theta/2} \sin\alpha\cos\alpha e^{jB\sin\alpha}d\alpha,$$

$$E_\theta(\theta) = \left(\cos^2\frac{\theta}{2}\right)I_1 - \left(\frac{\sin\theta}{2}\right)I_2. \quad (28)$$

The first integral, I_1, is quite difficult to evaluate, but by dropping the $\theta/2$ term from the limits of integration, it can be expressed as follows

$$I_1 = \int_{-\pi/2}^{\pi/2} \cos^2\alpha e^{jB\sin\alpha}d\alpha = \int_{-\pi/2}^{\pi/2} \cos^2\alpha\cos(B\sin\alpha)d\alpha + j\int_{-\pi/2}^{\pi/2} \cos^2\alpha\sin(B\sin\alpha)d\alpha.$$

The integrand in the second integral above is an odd function, so the value of the integral is zero. The integrand in the first integral is an even function, so it may be written as

$$I_1 = 2\int_0^{\pi/2} \cos^2\alpha\cos(B\sin\alpha)d\alpha,$$

$$I_1 = \int_0^{\pi/2} \cos(B\sin\alpha)d\alpha + \int_0^{\pi/2} \cos 2\alpha\cos(B\sin\alpha)d\alpha,$$

$$I_1 = \frac{\pi}{2}[J_0(B) + J_2(B)]. \quad (29)$$

For values of θ up to 6°, which is sufficient to include the first two side lobes, the error introduced by neglecting $\theta/2$ in the limits of I_1 can be shown to be less than 0.004 per cent of $(I_1)_{max}$. The second integral, I_2, in (28) can be integrated directly to give

$$I_2 = \frac{2j}{B^2}\left[\sin\left(B\cos\frac{\theta}{2}\right) - B\cos\frac{\theta}{2}\cos\left(B\cos\frac{\theta}{2}\right)\right]. \quad (30)$$

Substituting (29) and (30) into (28), the normalized radiation pattern for the E-plane given in the text as (8) is then

$$E_\theta(\theta) = \cos^2\frac{\theta}{2}[J_0(B)+J_2(B)] - j\frac{2\sin\theta}{\pi B^2} \cdot\left[\sin\left(B\cos\frac{\theta}{2}\right) - B\cos\frac{\theta}{2}\cos\left(B\cos\frac{\theta}{2}\right)\right]. \quad (8)$$

H-Plane Pattern

For the H-plane pattern, the far-field point P is confined to the xz-plane where $\phi = 0$ or 180°, but due to symmetry about this plane only one value of ϕ need be considered. Inspection of (17) and (18) for $\phi = 0$ shows

$$\vec{\rho}\cdot\hat{R}_1 = x\sin\theta + r_0\cos\psi\cos\theta.$$

Then (24) and (25) may be written

$$E_\theta(\theta) = \sin\theta\int_{-t/2}^{t/2} \cos\frac{\pi x}{t}e^{jkx\sin\theta}dx\int_{-\pi/2}^{\pi/2} \sin\psi\cos\psi \cdot e^{-2jkr_0\cos\psi\sin^2\theta/2}d\psi, \quad (31)$$

and

$$E_\phi(\theta) = (1+\cos\theta)\int_{-t/2}^{t/2} \cos\frac{\pi x}{t}e^{jkx\sin\theta}dx\int_{-\pi/2}^{\pi/2} \cos^2\psi \cdot e^{-2jkr_0\cos\psi\sin^2\theta/2}d\psi. \quad (32)$$

Equation (31) involves an integral of an odd function from $-\pi/2$ to $\pi/2$, and is therefore zero. The first integral in (32) is given by

$$\int_{-t/2}^{t/2} \cos\frac{\pi x}{t}\, e^{jkx\sin\theta}dx = \frac{\frac{2t}{\pi}\cos\left(\frac{kt\sin\theta}{2}\right)}{1-\left(\frac{kt\sin\theta}{\pi}\right)^2}. \quad (33)$$

For the second integral, the substitution $D=2kr_0\sin^2(\theta/2)$ gives an integral which was worked out by McLachlan[15] in terms of Bessel and Struve functions[16] as

$$\int_{-\pi/2}^{\pi/2} \cos^2\psi e^{-jD\cos\psi}d\psi = \pi\left[\left\{J_0(D)-\frac{J_1(D)}{D}\right\} - j\left\{H_0(D)-\frac{H_1(D)}{D}\right\}\right]. \quad (34)$$

Then, combining (32), (33), and (34), the normalized H-plane pattern given in the text by (9) is

$$E_\phi(\theta) = \left[\frac{\frac{(1+\cos\theta)}{2}\cos\left(\frac{kt\sin\theta}{2}\right)}{1-\left(\frac{kt\sin\theta}{\pi}\right)^2}\right] \cdot \left[\left\{J_0(D)-\frac{J_1(D)}{D}\right\} - j\left\{H_0(D)-\frac{H_1(D)}{D}\right\}\right]. \quad (9)$$

[15] N. W. McLachlan, "Bessel Functions for Engineers," p. 83, Ex. 27, The Clarendon Press, Oxford, England; 1934.
[16] Tabulated in E. Jahnke, and F. Emde, "Tables of Functions," 4th ed., Dover Publications, New York; 1945.

The Effect of Ions on Magneto-Ionic Characteristic Polarization

W. SNYDER†, ASSOCIATE, IRE

Summary—**There is some evidence for the presence of large numbers of ions in the *E*-region. Considering the recent increase in the precision with which sky-wave polarization measurements can be made, it seems desirable to fill a gap in the usual magneto-ionic theory by investigating the effect on the theoretical characteristic polarizations of introducing a mixture of ions and electrons into the calculations. A general formula is derived as an extension of the magneto-ionic polarization expression of Goubau.**

The 100 kc and 300 kc polarizations predicted by this formula have been plotted for a neutral mixture of oxygen ions, nitrogen ions, and electrons. The plots show that polarizations are possible in a mixture that cannot occur when only electrons are present. They also show that characteristic polarizations in a mixture do not define the medium parameters as completely as they do with electrons only. Another interesting feature is that the polarizations in a mixture depend on the relative numbers of each type of charged particle but seem not to depend on the actual charge density when the proportion of electrons is small.

RECENT PAPERS indicate that there may be rather large concentrations of ions in the *E* layer.[1,2] Usual magneto-ionic theory neglects the effect of ions and considers only that of electrons as being important. Surely, if there are equal numbers of ions and electrons this is a valid procedure, since ions are so much heavier than electrons. However, if the ions are much more numerous than the electrons they can have an appreciable effect on the polarization.

G. Goubau[3] has treated the ion-electron mixture extensively in terms of the propagation constant. He gives an expression for the polarization in a general mixture for zero heavy ion and electron densities, and an expression for the polarizations for any ion density when the electron density is considerable. He shows that in the latter case the electrons chiefly determine the characteristic polarizations.

For the limiting polarization case, he points out that the polarizations vary widely depending on the type and proportions of ions comprising the mixture. A general expression for polarization is not given nor is there any discussion of what would happen for any specific choice of ions except that if the positive and negative ions were of equal charge to mass ratio and equal number, the characteristic polarizations would be linear with tilt angles of zero and 90° with respect to the component of magnetic field in the phase front.

It seems desirable, now that precise polarization measurements are being made, to consider in a little more detail what some fairly reasonable mixture of ions and electrons will do to the theoretical characteristic polarizations. To this end, one should have a general expression for polarization in an arbitrary mixture for any ionization densities.

Such an expression was derived following the same general method indicated by Goubau. That is to say, Maxwell's equations were written for the field with the conduction current term taken to be $\sum_i N_i e_i \vec{V}_i$ where N_i is the number of ith type ions per cubic meter, e_i charge on ith type ions and V_i is velocity of ith type ions. A force equation for each type ion was written

$$m_i\frac{d\vec{V}_i}{dt} = e_i(\vec{E}+\vec{V}_i\times\vec{B}_E) - m_i\nu_i\vec{V}_i \quad (1)$$

† Stanford University, Stanford, Calif.
[1] J. C. W. Scott, *Jour. Geophys. Res.*, vol. 56, no. 1, p. 1; March, 1951.
[2] J. C. Seddon, Program abstracts of May 5–7, 1952, meeting of American Geophysical Union, p. 322, abstract no. 17.
[3] C. Goubau, *Hochfreq. und Electroak.*, vol. 46, pp. 37–49; August, 1935.

where m_i is the mass and ν_i the collision frequency of the ith type ion. E is the radio frequency electric field and B_E is the earth's magnetic field flux density. This treatment neglects restoring forces proportional to particle displacement.

After half a dozen pages of tedious algebra, the expression for polarization, Q, was obtained as

$$Q_{1,2} = \frac{B_T^2[c^2 - (1+a)d]}{2B_L c[1+a+B_E^2 d]} \pm \sqrt{\left\{\frac{B_T^2[c^2-(1+a)d]}{2B_L c[1+a+B_E^2 d]}\right\}^2 - 1} \quad (2)$$

where

$$a = \sum_i \left(\frac{x_i(1-jz_i)}{y_i^2-(1-jz_i)^2}\right)$$

$$c = \sum_i \left\{-j\,\frac{x_i y_i}{B_E(1-jz_i)(y_i^2-[1-jz_i]^2)}\right\}$$

$$d = \sum_i \left\{\frac{-x_i y_i}{B_E^2(1-jz_i)(y_i^2-[1-jz_i]^2)}\right\}$$

$$x_i = \frac{N_i e_i^2}{\epsilon_0 m_i \omega^2}$$

$$y_i = \frac{B_E e_i}{m_i \omega}$$

$$z_i = \frac{\nu_i}{\omega}$$

ν_i = collisional frequency of the ith type ion
ω = signal angular frequency (2πf)
N_i = number of ith type ions per cubic meter
e_i = charge on ith type ion
m_i = mass of ith type ion
B_E = flux density of earth's magnetic field (MKS)
B_t = transverse component of B_E
B_L = longitudinal component of B_E
ϵ_0 = dielectric constant of free space (MKS)
$Q = Hz/Hy$ where Hy is the magnetic component of signal perpendicular to plane determined by B_E and direction of propagation, Hz is the component in plane. In an x, y, z, coordinate system, x is the direction of propagation. (See Fig. 1.)

In the limit $x_i \to 0$, (1), agrees with Goubau and if only electrons are considered it becomes the usual magneto ionic polarization expression.

If we write

$$\frac{1}{Z+jX} = \frac{B_T^2[c^2-(1+a)d]}{2B_L c[1+a+B_E^2 d]}$$

then

$$Q_{1,2} = \frac{1}{Z+jX} \pm \sqrt{\left(\frac{1}{Z+jX}\right)^2 - 1}. \quad (3)$$

Equation (3) has been plotted in detail for $Q=\alpha+j\beta$ with Z and X as parameters and also for ratio of minor to major axis versus tilt of major axis of the ellipse represented by Q with the same Z and X as parameters.[4] To see the behavior of the ellipse we need only solve for Z and X and then, from the plots mentioned, pick off the appropriate Q or ellipse. Unlike the case with only one type of charged particle, both Z and X are functions of both x_i and z_i and the relationships are such that in the general case considered here, no simple normalization could be found but, instead, special cases had to be computed. From these special cases, however, it is felt that the effect of ions is fairly clear.

If we require that the ionosphere be electrically neutral, we must consider only cases in which there are as many negative as positive charges. The most likely situation is one having both positive and negative ions, but with ions of one sign possessing a higher charge-to-mass ratio than the other. A fairly reasonable model might be one in which there were free electrons, nitrogen molecules with one electron missing, and oxygen molecules with one electron added. Using Goubau's mixture coefficient, K, for this mixture we have

$$K = \frac{x_1}{x_2 + x_3}$$

where the subscript 1 refers to electrons, the 2 refers to nitrogen molecules and the 3 to oxygen molecules.

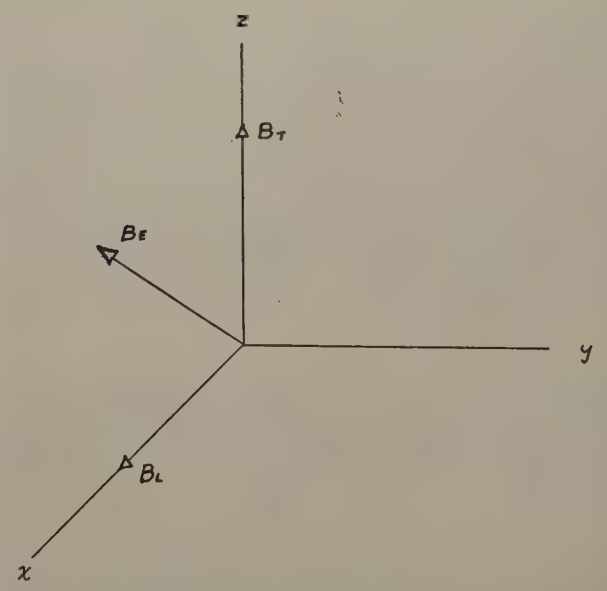

Fig. 1—Coordinate System (Propagation in $+x$ direction).

We can obtain some insight into the effect of ions by calculating polarizations as a function of K keeping $x_1+x_2+x_3$ constant for particular cases of signal frequency, magnetic dip angle, collisional frequency, and gyro frequency. $Z+jX$ for the cases of $f=300$ kc, $x_1+x_2+x_3=0$ and 0.5, $z_1=0.27$ and 1.06 are tabulated in

[4] W. Snyder, and R. A. Helliwell, *Jour. Geophys. Res.*, vol. 57, no. , p. 73; March, 1952.

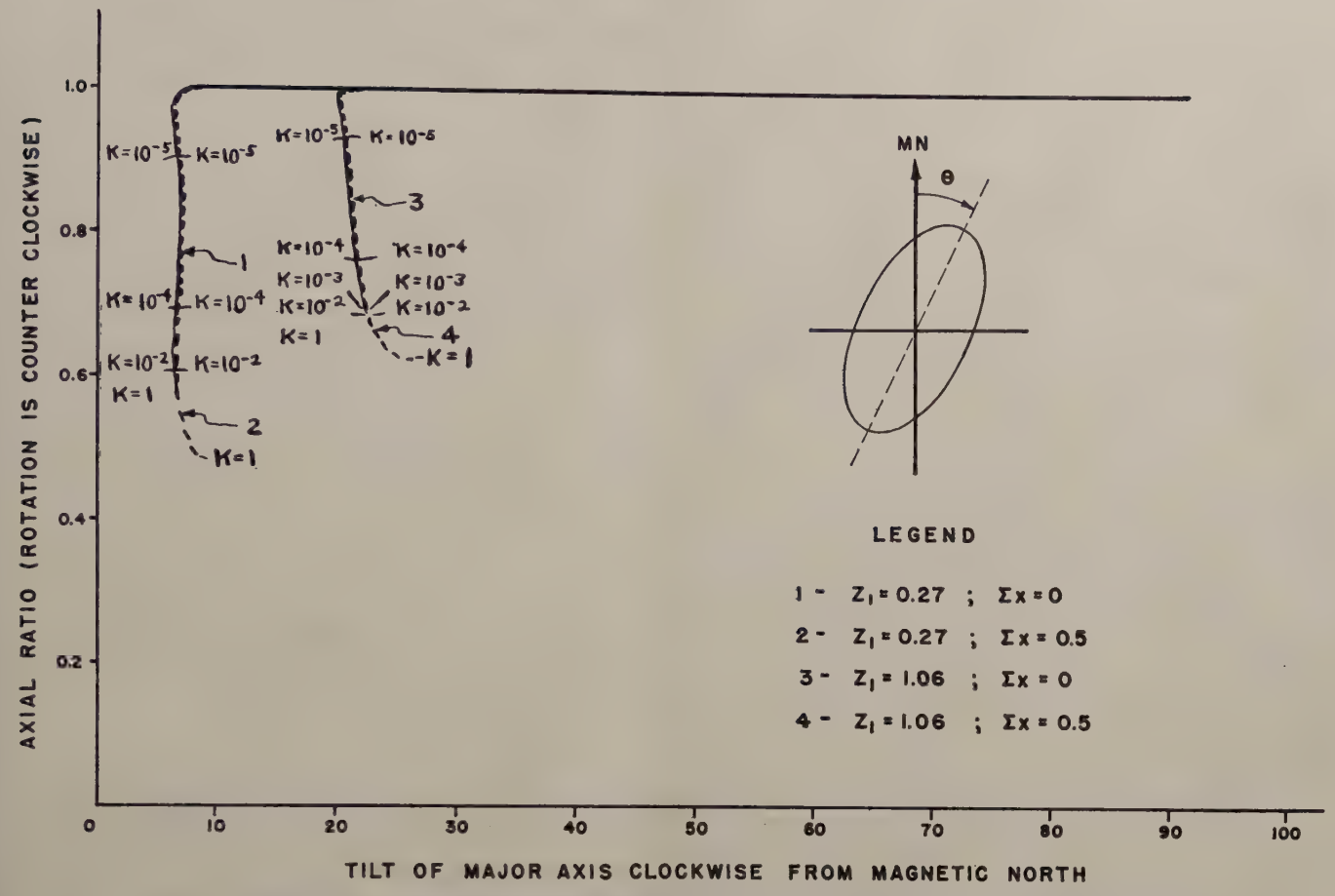

Fig. 2—Polarization of one downcoming magneto-ionic component vs. K at 300 kc looking in the direction of propagation in the northern hemisphere.

TABLE I
$Z+jX$ vs. K at 300 kc

K	$x_1+x_2+x_3=0$ $z_1=1.06$	$x_1+x_2+x_3=0.5$ $z_1=1.06$	$x_1+x_2+x_3=0$ $z_1=0.27$	$x_1+x_2+x_3=0.5$ $z_1=0.27$
1	1.964+j1.851	1.940+j1.208	0.4910+j1.8506	0.4923+j1.234
10^{-1}			0.49113+j1.8514	
10^{-2}	1.972+j1.862	1.972+j1.843	0.4929+j1.859	0.4925+j1.859
10^{-3}	2.044+j1.959	2.044+j1.957		
10^{-4}	2.768+j2.932	2.768+j2.932	0.6821+j2.731	
10^{-5}	9.398+j11.94	9.398+j11.94	2.405+j10.66	
10^{-6}	83.58+j110.3	83.58+j110.3	19.84+j90.42	18.56+j84.61
10^{-7}	941.5+j1,116.5	922.2+j1,212		
10^{-8}	−5,833−j21,501	21,220−j9,751	11,088+j18,794	
0	−191.8−j14,013	−3,467−j13,953	−49.691−j14,542	−54.1−j14,205

Table I and the corresponding polarization ellipses plotted in Fig. 2.

$Z+jX$ for the cases of $f=100$ kc, $x_1+x_2+x_3=0$, $z_1=0$, 1, and 3.2 are tabulated in Table II and the ellipses plotted in Fig. 3.

In all cases an electron gyro frequency of 1.3 mc and a magnetic dip angle of 62° is assumed. The collisional frequencies of nitrogen and oxygen ions are taken to be $\nu_2=1/40\nu_1$ and $\nu_3=1/43\nu_1$, respectively, following Goubau.

Two cases of limiting polarization at 7 mc were calculated, one for $K=10^{-3}$ (K drops out of the expression if it is greater than 10^{-3}) and the other for $K=0$. The polarization at 7 mc was circular for the two limits of K so no further calculations were made as the trend of the curves indicates that in all cases the limiting polarizations at 7 mc are circular.

As can be seen from the plots and tables, the trend of all the cases plotted is the same. That is, for values of K greater than about 10^{-2} the polarization is very close to

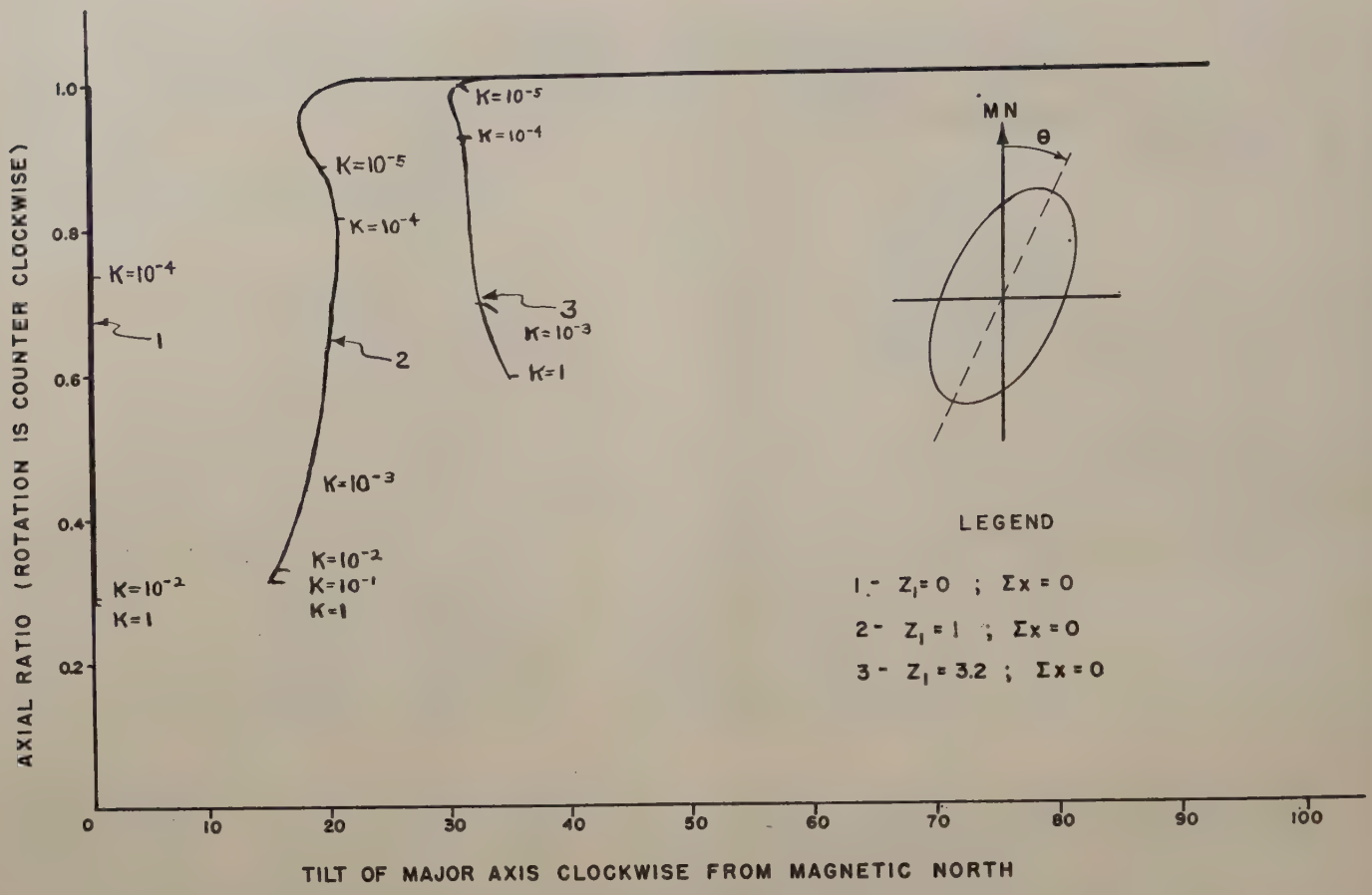

Fig. 3—Polarization of one downcoming magneto-ionic component vs. K at 100 kc looking in the direction of propagation in the northern hemisphere.

TABLE II

$Z+jX$ vs. K at 100 kc

K	$x_1+x_2+x_3=0$ $z_1=0$	$x_1+x_2+x_3=0$ $z_1=1$	$x_1+x_2+x_3=0$ $z_1=3.2$
1		0.616+j.616	1.96+j0.616
10^{-1}	0+j.6186	0.619+j.619	
10^{-2}	0+j.6433	0.642+j.646	
10^{-3}		0.875+j.914	2.79+j1.10
$5(10)^{-4}$		1.13+j1.21	
10^{-4}	0+j3.336	3.21+j3.61	10.23+j5.459
$5(10)^{-5}$		4.89+j6.46	18.53+j10.28
10^{-5}		29.4+j30.6	86.1+j48.1
10^{-6}		293+j300	1,030+j372
10^{-7}		601−j48.2	2,680−j5,059
0	0−j4,810	−62−j4,890	−193−j4,281

that determined by the electrons only, but as K decreases (proportion of ions increases) the ellipse tends to become more circular and the tilt angle changes. For very small K the ellipse is essentially circular and although as K approaches zero the tilt increases, finally getting into the "forbidden" quadrant for electrons, the ellipse is so nearly circular that the tilt angle is not observable.

One result that comes out of this is that some polarizations, impossible in a medium which has only electrons as the charged particles, are possible when ions are present. In fact, all the limiting polarizations (again defined here as those corresponding to all $x_i=0$) in a mixture could be accounted for only by negative densities of electrons alone. Thus, if polarizations were observed which would indicate negative electron densities, it would not necessarily mean that magneto-ionic theory did not apply; it could mean that the medium contained a mixture of ions and electrons.

In addition, one can say from the fact that curves of constant collisional frequency for which $\sum x_i=0.5$ and those for which $\sum x_i=0$ essentially overlap for most of their length that a given polarization does not uniquely determine K or $\sum x_i$ in general.

On the other hand, this overlap shows that collisional frequency could be obtained in principle from a polarization observation of a magneto-ionic component if conditions were such that magneto-ionic theory were applicable. The procedure for doing it would be cumbersome. It would consist of plotting curves for a family of collisional frequencies and then interpolating for the values of collisional frequency corresponding to the observed polarization.

Table I shows most clearly the extent of the overlap for different $\sum x_i$. For the range of $K<10^{-2}$ or so, for which the polarizations are not circular, the polarizations for $\sum x_i=.5$ and $\sum x_i=0$ seem to be the same if K is the same.

It should be emphasized in concluding, that for the effects of ions to be discernible in polarization measurements, the relative number of ions as compared to electrons must be enormous. The quantity K may be writen for the mixture discussed as

$$K = \frac{N_1/m_1}{N_2/m_2 + N_3/m_3} \tag{4}$$

where $m_2/m_1=51{,}200$, $m_3/m_1=59{,}200$ and since $N_2=N_3$ very closely for values of K considered, we may write

$$K = \frac{N_1}{N_2}\left(\frac{1}{m_1/m_2 + m_1/m_3}\right)$$

$$\text{or } K = \frac{N_1}{N_2}3(10)^4$$

$$\text{or } K = \frac{N_1}{N_2+N_3}\times 6(10)^4 \text{ since } 2N_2 = N_2 + N_3, \tag{5}$$

so that if $K=1$, $N_2+N_3=6(10)^4 N_1$.

It is seen that for this value of K the limiting polarization is essentially that due to electrons only. In fact, the ions do not begin to affect the polarizations much until they outnumber the electrons about six million to one. This is a much less sensitive quantity for detecting ions than is the critical frequency separation. According to Goubau, the conditions for reflection in a mixture are

$$x_1 + x_2 + x_3 = 1$$

$$\frac{x_1}{1+y_1} + x_2 + x_3 = 1. \tag{6}$$

We may write $x_1=\omega_1^2/\omega^2$, so that, if $\omega_m{}^0$ is ordinary critical frequency in the mixture and $\omega_m{}^x$ is extraordinary critical frequency,

$$\omega_1^2 + \omega_2^2 + \omega_3^2 = \omega_m{}^{0^2}$$

$$\frac{\omega_1^2}{1+y_1} + \omega_2^2 + \omega_3^2 = \omega_m{}^{x^2}$$

$$\omega_1^2\left(1 - \frac{1}{1+y_1}\right) = \omega_m{}^{0^2} - \omega_m{}^{x^2} = \omega_1^2\left(\frac{y_1}{1+y_1}\right). \tag{7}$$

Now

$$K = \frac{\omega_1^2}{\omega_2^2 + \omega_1^2}.$$

Hence

$$\omega_1^2(1 + 1/K) = \omega_m{}^{0^2},$$

and, in terms of the ordinary critical frequency,

$$\omega_1^2 = \frac{K\omega_m{}^{0^2}}{K+1}.$$

Thus

$$\omega_m{}^{0^2} - \omega_m{}^{x^2} = \frac{K\omega_m{}^{0^2}}{K+1}\left(\frac{y_1}{1+y_1}\right),$$

so that, for $K=1$, the separation is changed by a factor of 1/2, for the same ordinary critical frequencies in a mixture, in comparison with the pure electron case, even though the polarizations are not changed. However, the 0 and x waves may be reflected from different heights where different K's prevailed. In fact, the reflection is likely to occur at a place of few ions, but the polarizations may be determined in a lower region where ions are more likely. The figures given by Seddon[2] show that a ratio of $(N_2+N_3)/N_1=2.8(10)^5$ at least exists at 90 km, corresponding to $K=2(10)^{-1}$. K could have been much smaller since this value of K is based on N_1 being just below the minimum detectable.

Since N_1 could have been much smaller this shows that the effect of ions on the polarizations may have to be taken into consideration in interpreting polarization experiments.

Acknowledgment

The author wishes to acknowledge the financial assistance of the National Bureau of Standards during the course of this work and the helpful comments and suggestions of R. A. Helliwell of Stanford University.

Bibliography

1. D. A. Campbell, "A Low Frequency Polarimeter," Technical report issued by Electronics Research Laboratory, Stanford University, Stanford, Calif.; prepared under Bureau of Standards Contract CST-10751; August 1, 1951.
2. M. G. Morgan, "Polarization control and measurement in ionosphere vertical incidence echo ranging," *IRE Professional Group on Antennas and Propagation*, PGAP-3, pp. 33–41; August, 1952.
3. E. L. Kilpatrick, "Polarization measurements of low frequency echoes," *Jour. Geophys. Res.*, vol. 27, no. 2, p. 221; June, 1952.
4. H. J. Nearhoof, Basic Ionosphere Research Technical Report No. 25, Ionosphere Research Laboratory, The Pennsylvania State College, AMC Contract No. AF19(122)-44; August 20, 1951.

communications

The 1953 Symposium on Tropospheric Wave Propagation Within the Horizon at the U.S. Navy Electronics Laboratory

W. C. HOFFMAN*

Summary—**A symposium on "Tropospheric Wave Propagation Within the Horizon" was convened at the U. S. Navy Electronics Laboratory during March 30–April 2, 1953, under the chairmanship of Dr. Charles R. Burrows. There were three sessions, devoted respectively to the effects of rough terrain, to the effects of atmospheric refraction and to propagation phenomena arising from combination of these effects.**

THE SESSION ON terrain effects was about evenly divided between the reporting of experimental results and exploring theoretical methods for solving the electromagnetic field over a rough boundary. Mr. W. S. Ament outlined three possible approaches to the latter: (1) the equivalence between wave propagation over a rough surface and propagation through a "blobby" medium; (2) approximation of the rough surface by an infinite set of parallel plates with random spacing; and (3) the application of noise statistics. Mr. W. C. Hoffman spoke on the approach that has been attempted at NEL, consisting of solution of an integral equation for the surface currents together with application of some recently developed results of probability theory.

Dr. Victor Twersky described his work on reflection of electromagnetic waves from a striated surface, using the model of an infinite set of randomly spaced semi-cylindrical bosses on a perfectly conducting plane. He finds that multiple scattering can be neglected with such a model at all angles of incidence for horizontal polarization. For grazing incidence the model behaves like a perfect reflector regardless of polarization or the dielectric properties of the bosses. An interesting result is that approximations for reflection coefficients and differential scattering cross-sections which conserve energy may be found by retaining only the leading term of an expansion in terms of $1/k\bar{b}\cos\alpha$ (where $\bar{b}$ is the average separation of neighboring scatterers and α is the angle of incidence) provided $k\bar{b}\cos\alpha \gg 1$. For grazing incidence, however, this approximation breaks down and multiple scattering must be taken into account. When the radius of the cylinders is large with respect to wavelength a polar plot of the reflected radiation is roughly semi-circular except for a sharp spike in the specular direction. The back scattering cross section in the case of horizontal polarization behaves essentially the same whether the radius is large or small with respect to wavelength.

Mr. H. W. Smith gave a paper entitled "Power Spectrum Estimates of Radio Waves and Simultaneous Sea State for An Overwater Path." The Tukey method was used in estimating the power spectra. There was reasonable agreement between the power spectra of radio field and sea state at centimeter wavelengths but not at millimeter wavelengths. A paper by L. G. Trolese and J. P. Day, "Diffraction Effects on an Optical Short Wave Link," described the pronounced enhancement by night-time refraction of knife-edge diffraction from a small hill about a half-mile in front of the receiving antenna. The possibility of strong local propagation effects from portions of an optical path in the neighborhood of the antenna was also brought out in K. Bullington's paper on "Reflection Coefficients of Irregular Terrain." Over one path a change from 16 to 11 db in the depth of the null resulted from moving the receiving antenna laterally a hundred feet. A plot of reflection coefficient versus roughness parameter for a number of paths across the United States showed no particular correlation between the two, the mean reflection coefficient being 0.28 at 4000 mc.

* U. S. Navy Electronics Lab., San Diego 52, Calif.

Mr. A. P. Barsis reported on "Tropospheric Propagation Measurements within the Radio Horizon—Cheyenne Mountain Path." This is an optical path in Colorado essentially duplicating air-to-ground propagation. A least squares fit of the terrain over that portion of the path within line-of-sight of the receiving antenna was used to give an effective earth's radius and smooth-earth theory then applied. Rayleigh's roughness criterion in terms of the mean deviation of "fitted" from "true" terrain height was computed. It was found that when the criterion was small, the measured field exceeded the computed field; when it was large, the computed field was the larger. Dr. H. W. Swarm described some VHF measurements over extremely rough terrain in the Seattle area and a method of computing the field on the basis of reflected, refracted and diffracted components.

Dr. J. B. Smyth led off this session with a comparison between a link partially over water from Mt. Wilson to San Diego, thus simulating air-to-ground propagation, and one wholly over water from San Pedro to San Diego. There was no apparent relation between instantaneous signal levels on the two links. Mr. J. P. Day then discussed a paper titled, "Propagation Characteristics of Microwave Optical Links," concerning fades on links in the vicinity of San Diego, San Francisco, and Norfolk. On one occasion the height-gain curve for the San Diego link under trapping conditions was such that maxima under standard conditions became minima and vice versa. Thus a receiving antenna located at a normal maximum of the height-gain curve would show a deep fade. The shift in the height-gain curve could be computed on the basis of an effective earth's radius of -2. From a continuous record of field strength it was also found that there was a fading period of approximately 14 seconds coinciding closely with the period of ocean swells originated by southern hemisphere storms. Of the two paths in the San Francisco area, one had a strong ground-reflected component and exhibited deeper fades than the other. The Norfolk link was notable for the number of lengthy "flat bottom" fades observed there, some of which were associated with frontal passages.

Dr. L. H. Doherty gave a paper on "The Effect of Atmospheric Ducts on Line-of-Sight Transmission" in which he developed ray theory for optical transmission for various types of ducts and various transmitter heights and proposed supplementing ray-tracing by use of the Airy integral in the neighborhood of caustics. Mr. Wong described the work at the Aircraft Radiation Laboratory in ray-tracing in a paper, "Correlation of Radio Holes and Fading Regions with Calculations." Ray tracing with a REAC gives a graphic display of radio-holes for a number of transmitter heights and a stratified atmosphere or linear refractive index profile. The location of the radio-holes is quite sensitive to transmitter height. It is hoped to employ Freehafer's method and the REAC in a more general wave treatment.

There were a number of comments on the ray-tracing approach, which may perhaps best be summed up in the statement that the method has practical value but does need to be supplemented in regions near cusps and caustics. To have complete correspondence between theory and practice it is necessary to know much more than we do about the meteorology of progressive change in the refractive index profile in time and space and, in some situations, to take into account the ground-reflected ray.

The session on refraction was marked by a lively controversy between the advocates of ray-tracing methods for determination of "radio holes," on the one hand, and the proponents of multipath and focusing-defocusing effects as explanations of fading on optical links, on the other. The matter of eventually explaining and/or predicting fades on optical communication links (and radio-holes in the case when one or both terminals are airborne) was probably the main goal of the session.

Mr. Bullington then described the experiments of Crawford and Jakes (BSTJ; January, 1952) on fading on optical links caused by multipath transmission and showed some highly interesting films of the behavior of the received pulses. There was a lively discussion of the explanation of the observed phenomena.

Mr. P. Chavance then described his observations on a grazing microwave link in the north of France. The median signal fell between the values for diffraction by a spherical earth and diffraction by a knife edge. There were marked diurnal and seasonal trends in the frequency of deep fades. It was notable that interference type fades could be explained on the basis of two rays of nearly equal amplitude and a third ray of much smaller amplitude, whose relative phases are slowly varying linear functions of time. Mr. Chavance also described a new link consisting of two convergent paths over the Mediterranean, from which he expects to have some interesting data shortly. Dr. C. C. Aurell spoke on fading observed at 3.5 cm on an optical overwater path in the Baltic. Space diversity reception was employed with one receiver situated at a height-gain maximum for a 4/3 earth and the other at a minimum. Two different types of fades were observed. The first consisted of deep fades on both receivers with no apparent correlation, the second, of low signal on one receiver but strong reception on the other. The first type may be attributed to convergence of the reflected ray (so that its amplitude is approximately that of the direct ray) together with a third component reflected from an elevated layer. He also has noted that deep fades on overwater paths are often associated with frontal conditions.

It seemed to be the concensus that the variation in optical fields is due to either multipath transmission or focusing-defocusing, and it was suggested by Dr. Smyth that the focusing-defocusing effect would appear to have a different frequency dependence than the multipath, so that this might provide a means of distinguishing experimentally between causes of fades.

Mr. W. E. Gordon gave a paper on "Radio Scattering on Optical Paths," which is an extension of the Booker-Gordon theory of turbulent scattering to the case of large blobs (of the order of 10–50 meters) and short paths (30–60 kilometers). These new features necessitate taking account of the non-uniform illumination of the blobs and of the searchlight portion of the scattering polar diagram. The theory is not intended to apply to deep fades but only to the small scintillations on an otherwise steady signal and, as such, points a way to determining the scale of turbulence experimentally through measurements of the three parameters: fading amplitude, fading rate and correlation distance.

Mr. A. P. Barsis described some measurements on fading over two optical links in Eastern Colorado, the fades being of the flat-bottom type. His observations also exhibited pronounced diurnal and seasonal trends in frequency of occurrence, and the fades were much more frequent and severe on 1046 mc than on 100 or 192.8 mc. Mr. Doherty showed how flat-bottom fades might be due to a radio hole. An alternative explanation for the fades observed by Mr. Barsis was suggested by Mr. L. J. Anderson. Night-time drainage of cold air down a valley in front of the farthest receiver could provide a reflecting surface and thus give a reflected component annulling the direct ray. For the nearer receiver the local terrain was such that a substandard condition could be produced by moisture condensation and it was pointed out that such a condition would have a much greater effect at the higher frequency, in accord with the observations. A final paper, "Summary of A.P.O Microwave Propagation Measurements on Sydney-Melbourne Route," by Mr. J. H. Reen was read by title, describing some fades apparently due to substandard conditions

INSTITUTIONAL LISTINGS

The IRE Professional Group on Antennas and Propagation is grateful for the assistance given by the firms listed below, and invites application for Institutional Listing from other firms interested in the field of Antennas and Propagation.

THE GABRIEL LABORATORIES, 135 Crescent Road, Needham Heights, Massachusetts
Research and Design of Antenna Equipment for the Workshop Assoc. and Ward Products Div. of the Gabriel Co.

POLYTECHNIC RESEARCH AND DEVELOPMENT COMPANY, INC., 55 Johnson Street, Brooklyn 1, New
Microwave Precision Test Equipment—Design, Development, Production.

WHEELER LABORATORIES, INC., 122 Cutter Mill Road, Great Neck, New York
Consulting Services, Research and Development, Microwave Antennas and Waveguide Components.

The charge for an Institutional Listing is $25.00 per issue or $75.00 for four consecutive issues. Application for listing may be made to the Technical Secretary, The Institute of Radio Engineers, 1 East 79th Street, New York 21, New York.